This copy is for personal use only. To order printed copies, contact *reprints@rsna.org*

Imaging of Renal Transplant Complications throughout the Life of the Allograft: Comprehensive Multimodality Review

Mark D. Sugi, MD
Gayatri Joshi, MD
Kiran K. Maddu, MD
Nirvikar Dahiya, MD
Christine O. Menias, MD

Abbreviations: ATN = acute tubular necrosis, FDG = fluorodeoxyglucose, MAG_3 = mercaptoacetyltriglycine, MIP = maximum intensity projection, PTLD = posttransplant lymphoproliferative disorder, RI = resistive index

RadioGraphics 2019; 39:1327–1355

https://doi.org/10.1148/rg.2019190096

Content Codes: CT GU MR US

From the Department of Radiology, Mayo Clinic, Scottsdale, Ariz (M.D.S., N.D., C.O.M.); and Departments of Radiology and Imaging Sciences (G.J., K.K.M.) and Emergency Medicine (G.J., K.K.M.), Emory University School of Medicine, Atlanta, Ga. Recipient of a Certificate of Merit award for an education exhibit at the 2018 RSNA Annual Meeting. Received April 1, 2019; revision requested May 22 and received June 12; accepted June 17. For this journal-based SA-CME activity, the author N.D. has provided disclosures (see end of article); all other authors, the editor, and the reviewers have disclosed no relevant relationships. **Address correspondence to** G.J., Department of Radiology and Imaging Sciences, Emory University Hospital Midtown, 550 Peachtree St, Atlanta, GA 30308 (e-mail: *gayatri.joshi.md@gmail.com*).

©RSNA, 2019

SA-CME LEARNING OBJECTIVES

After completing this journal-based SA-CME activity, participants will be able to:

■ Describe the anatomic locations and vascular and urologic anatomy of the most commonly used renal transplant techniques and list the surgery-related, donor-related, and recipient-related factors that predispose to certain posttransplant complications.

■ Classify renal transplant complications according to time from surgery and recognize the distinguishing clinical findings as well as imaging findings at US and multimodality diagnostic imaging.

■ Discuss the role of imaging in guiding the multidisciplinary transplant team toward appropriate therapies in the setting of allograft rejection, infection, or malignancy.

See rsna.org/learning-center-rg.

The kidney is the most commonly transplanted solid organ. Advances in surgical techniques, immunosuppression regimens, surveillance imaging, and histopathologic diagnosis of rejection have allowed prolonged graft survival times. However, the demand for kidneys continues to outgrow the available supply, and there are efforts to increase use of donor kidneys with moderate- or high-risk profiles. This highlights the importance of evaluating the renal transplant patient in the context of both donor and recipient risk factors. Radiologists play an integral role within the multidisciplinary team in care of the transplant patient at every stage of the transplant process. In the immediate postoperative period, duplex US is the modality of choice for evaluating the renal allograft. It is useful for establishing a baseline examination for comparison at future surveillance imaging. In the setting of allograft dysfunction, advanced imaging techniques including MRI or contrast-enhanced US may be useful for providing a more specific diagnosis and excluding nonrejection causes of renal dysfunction. When a pathologic diagnosis is deemed necessary to guide therapy, US-guided biopsy is a relatively low-risk, safe procedure. The range of complications of renal transplantation can be organized temporally in relation to the time since surgery and/or according to disease categories, including immunologic (rejection), surgical or iatrogenic, vascular, urinary, infectious, and neoplastic complications. The unique heterotopic location of the renal allograft in the iliac fossa predisposes it to a specific set of complications. As imaging features of infection or malignancy may be nonspecific, awareness of the patient's risk profile and time since transplantation can be used to assign the probability of a certain diagnosis and thus guide more specific diagnostic workup. It is critical to understand variations in vascular anatomy, surgical technique, and independent donor and recipient risk factors to make an accurate diagnosis and initiate appropriate treatment.

©RSNA, 2019 • *radiographics.rsna.org*

Introduction

The kidney is the most commonly transplanted solid organ worldwide. In January 2019, there were 94 863 candidates on the waiting list for renal transplantation in the United States alone, according to the Organ Procurement and Transplantation Network (OPTN), compared with 61 488 in November 2004 (1,2).

The kidney donor risk index (KDRI), which incorporates donor-related factors such as demographics, medical history, and cause of death, can be used to estimate relative risk of graft failure. The kidney donor profile index (KDPI) remaps the KDRI onto a percentage scale that predicts graft failure, such that lower percentages are

TEACHING POINTS

- There are four main types of perinephric fluid collections commonly encountered in the renal transplant recipient: hematoma, urinoma, abscess, and lymphocele, occurring roughly chronologically in that order with respect to time from surgery.
- Reversed diastolic flow in the transplant renal artery at spectral Doppler US is highly suggestive of renal vein thrombosis but may also be seen less frequently with disorders such as allograft torsion, severe allograft rejection, or acute tubular necrosis. When reversed diastolic flow in the transplant artery is identified, the renal vein should be carefully interrogated to assess for renal vein thrombosis.
- In the absence of allograft dysfunction and secondary features of obstruction, it may be within acceptable limits to observe mild pelvicaliectasis due to the dependent orientation of the allograft in the iliac fossa and an increased tendency for vesicoureteral reflux. The increased tendency for vesicoureteral reflux is due to the relatively shorter length of the transplant ureter and loss of the normal obliquity and submucosal tunnel within the urinary bladder after ureteroneocystostomy.
- The types of bacterial, fungal, and viral infections that affect the renal transplant patient follow a relatively predictable pattern that correlates with the length of time from transplantation. However, the pattern of timing of infections may vary significantly, depending on factors like net state of immunosuppression at different time points and choice and duration of antimicrobial prophylactic agents.
- Malignancy is the third most common cause of death (after cardiovascular events and infection) in the renal transplant recipient, with three to five times the risk of malignancy as compared with the general population, with some cancers having markedly increased risk as high as 20–500-fold. Malignancy can occur as new malignancy in the recipient, as recurrent malignancy in the recipient, or as donor-related malignancy (transmitted to the recipient from the donor through the graft).

associated with longer estimated graft function. According to the OPTN, the number of deceased donor allografts with a KDPI of 86% or higher continues to grow each year, suggesting that kidneys with relatively higher risk of failure are being transplanted more frequently (3). Grafts with higher risk of failure by nature carry greater risk of allograft-related complications. Nevertheless, 1-year survival for patients with deceased donor renal allografts continues to improve over time, increasing from 87.7% in 1996 to 93.4% in 2014 (4,5).

With continued growing demand for renal transplantation, the role of the radiologist as a member of the multidisciplinary transplantation team continues to expand. Surveillance imaging and protocol biopsies are routinely performed during the first 1–2 years after transplant for detection of acute rejection and chronic allograft nephropathy, which may be clinically occult at the time of imaging or biopsy (6).

Duplex US is the principal modality used for evaluation of the renal allograft. A number of postoperative complications can be detected at US, including potentially correctable vascular abnormalities that may benefit from immediate reoperation to salvage the allograft. Among the many imaging findings of vascular disease, markedly decreased blood flow within the allograft at color and power Doppler assessment in the immediate postoperative period (within 4 hours of surgery) is the finding most associated with patient benefit from reoperation (7). Surveillance US includes assessment for hydronephrosis, perinephric fluid collections, and vascular patency and measurement of the intraparenchymal arterial resistive indexes (RIs) (8). Contrast-enhanced US may be useful when findings at surveillance US are indeterminate, particularly when distinguishing complicated cysts from solid renal masses. CT and MRI may be indicated in the setting of systemic disease or trauma.

Nuclear medicine may also play an important role in assessing both allograft perfusion and function, especially in the immediate postoperative period (9). Renal scintigraphy using radionuclides such as technetium 99m (^{99m}Tc) mercaptoacetyltriglycine (MAG_3) or ^{99m}Tc diethylenetriaminepentaacetic acid (DTPA) can provide both qualitative and quantitative information on cortical perfusion as well as parenchymal extraction and excretion, and may be particularly useful when used serially over time for comparison purposes (10). Special protocols using angiotensin-converting enzyme (ACE) inhibitors or diuretics may also be used when more specific diagnoses such as renal artery stenosis or obstruction, respectively, must be excluded (11).

Evidence-based practice guidelines for management of renal transplant recipients have been compiled by the Kidney Disease: Improving Global Outcomes (KDIGO) group, which includes recommendations for immunosuppression, antimicrobial prophylaxis, and treatment of complications (12). Implementation of these clinical guidelines, in conjunction with improvements in surveillance imaging and surgical techniques, has coincided with decreasing incidence of death-censored early graft failure (within the first 90 days of transplant) as well as graft failure or death at 5 years after transplant (13,14). Longer graft survival times may in turn be accompanied by increasing numbers of late complications such as interstitial fibrosis and tubular atrophy (chronic renal allograft nephropathy) and allograft malignancy, which tend to increase with the duration of follow-up (15).

In this article, we review the most frequently encountered as well as less common but important complications of renal transplantation and their typical imaging features. Following a

RadioGraphics

timeline from initial surgery, risk factors, clinical associations, and imaging findings are discussed.

Renal Transplant Technique

The surgical technique of renal transplantation may be tailored to anatomic characteristics unique to the donor kidney and factors related to the transplant recipient. The donor allograft may be right or left sided, or both in the case of en bloc kidneys. Variations in donor arterial, venous, and ureteral anatomy are important factors that influence the surgical technique and location of placement and may require special preparation of the allograft before transplantation. Influential recipient factors include prior abdominal surgery, vascular and urinary tract anatomy, and gender. The severity of underlying atherosclerotic arterial disease may favor one side over the other. Attention to the iliac vessels at preoperative imaging can help identify left iliac vein compression by the right common iliac artery (May-Thurner syndrome, which is more common in women) (16), allowing the surgeon to avoid left iliac fossa placement or take necessary therapeutic measures before left-sided transplantation.

Renal transplantation traditionally has been performed as an open operation; however, newer robot-assisted techniques for dissection, graft retroperitonealization, and venous, arterial, and ureterovesical anastomosis have been proposed as safe alternatives (17). In select patients, open abdominal surgery can also be avoided by using laparoscopic approaches for both donor nephrectomy and recipient surgery (18). The most common location for allograft placement is the right iliac fossa, owing in part to more frequent use of the left kidney as the donor allograft due to the relatively longer length of the left renal vein (19) (Fig 1). The left iliac fossa is often selected for second renal transplantation in the setting of a prior failed right iliac fossa allograft or during combined kidney-pancreas transplantation (20,21).

Simultaneous kidney-pancreas transplantation is an effective therapy for patients with diabetes mellitus complicated by end-stage renal disease and typically involves ectopic intraperitoneal placement of a pancreaticoduodenal allograft in the right iliac fossa and a renal transplant in the left iliac fossa. With respect to the pancreas transplant, venous drainage may be either systemic or via the portal venous system, with anastomosis of the donor portal vein to the recipient iliac vein or inferior vena cava, or to the recipient superior mesenteric vein, respectively (21).

Renal transplant arterial anatomy can vary considerably (Fig 1). In the case of deceased donor transplantation, the donor renal artery is frequently accompanied by a segment of donor aorta trimmed to an ovoid shape (Carrel aortic patch) and anastomosed to the recipient external iliac artery (EIA) in an end-to-side fashion (22,23). The Carrel aortic patch has the added advantage of potentially accommodating multiple arterial ostia, with a single end-to-side anastomosis (24). Accessory renal arteries are present in 30% of the population and are found bilaterally 10% of the time (25).

In the case of a living kidney donor, end-to-side anastomosis of the donor renal artery and recipient EIA is usually performed. End-to-end anastomosis with the recipient internal iliac artery is usually reserved for cases where the EIA has already been used for a prior transplant or where atherosclerotic disease of the EIA warrants an alternate anastomosis site (22,23,26). The donor renal vein is usually anastomosed to the recipient external iliac vein in an end-to-side fashion (22). En bloc transplantation of two smaller pediatric kidneys may also be performed, using the donor aorta and inferior vena cava to develop anastomoses with the external iliac vessels (27).

Number of (and distance between) multiple renal artery origins, presence of vascular disease, and en bloc transplantation of pediatric kidneys may require modifications in surgical technique, resulting in variations in postsurgical vascular anatomy. In living donor kidneys with multiple renal arteries, conversion to a single artery can be performed, which increases overall operative time but decreases operative time for anastomosis (28). It is important to identify and document the Doppler profile of each donor renal artery and vein at baseline postoperative US. In cases of uncertainty or variant anatomy, discussion with the transplant surgeon and attention to the operative notes can provide additional insight.

The transplant kidney ureter can be anastomosed to the recipient urinary bladder, often at the dome (ureteroneocystostomy), or alternatively to the recipient's native ureter after removal of the diseased native kidney using an end-to-side anastomosis (ureteroureterostomy), in cases where the length of the transplant ureter is insufficient or the recipient bladder anatomy precludes ureteroneocystostomy (29). Pyeloureterostomy is an additional technique that involves recipient nephrectomy with preservation of the recipient ureter, which is anastomosed to the donor renal pelvis (22,30).

Timeline of Renal Transplant Complications

Renal transplant complications can generally be categorized as early (which includes hyperacute and acute complications), intermediate, and late, depending on the time frame in which they

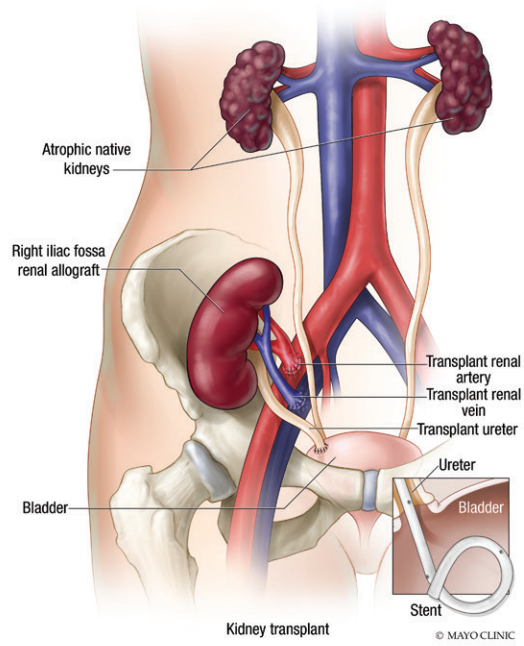

a.

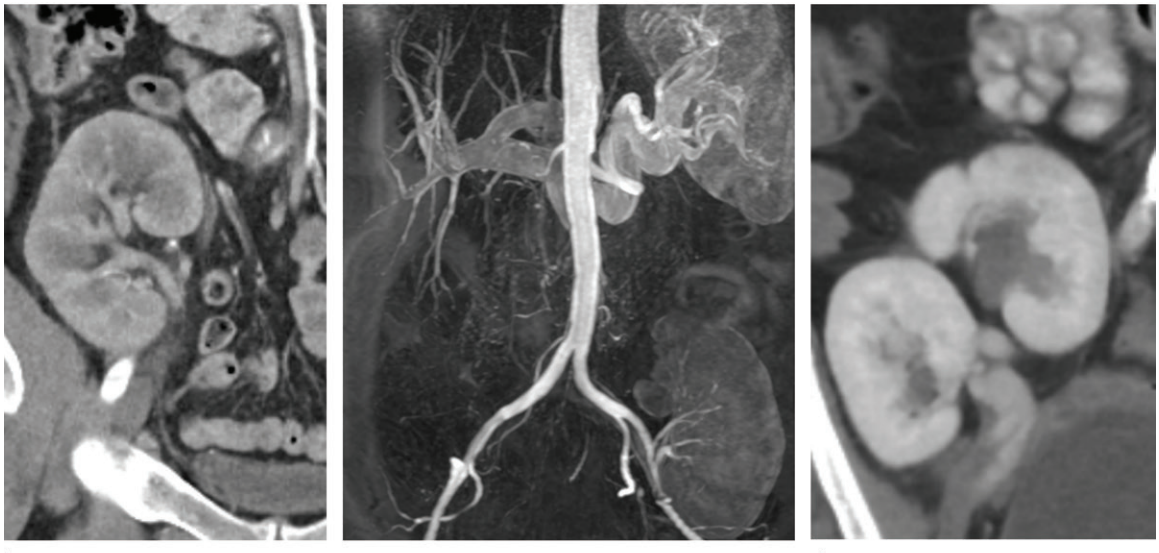

b. c. d.

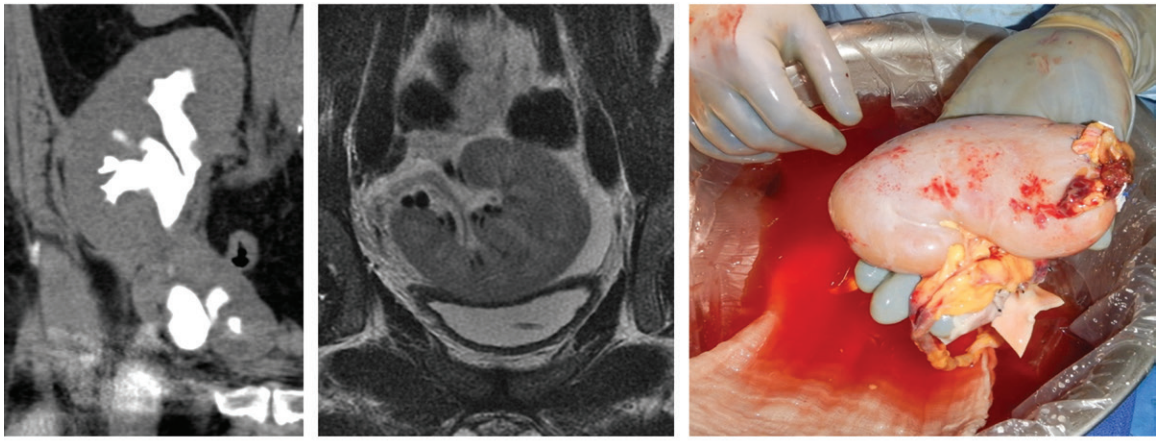

e. f. g.

Figure 1. Various types and locations of renal transplant. **(a)** Anatomic overview of the common right iliac fossa renal transplant. **(b)** Coronal contrast-enhanced CT image in the corticomedullary phase shows a single adult renal allograft in the right iliac fossa. **(c)** Coronal contrast-enhanced MIP (maximum intensity projection) MR image shows a renal transplant in the left iliac fossa. **(d)** Coronal contrast-enhanced CT image shows pediatric en bloc kidneys in the right iliac fossa. **(e)** Coronal CT image shows adult en bloc kidneys in the right iliac fossa with contrast material filling both renal collecting systems. **(f)** Coronal T2-weighted MR image shows atypical allograft placement, which can be warranted in cases of unique patient anatomy or vascular disease. **(g)** Photograph shows a deceased donor renal allograft before transplantation. Note that imaging does not allow distinction between living donor and deceased donor kidneys.

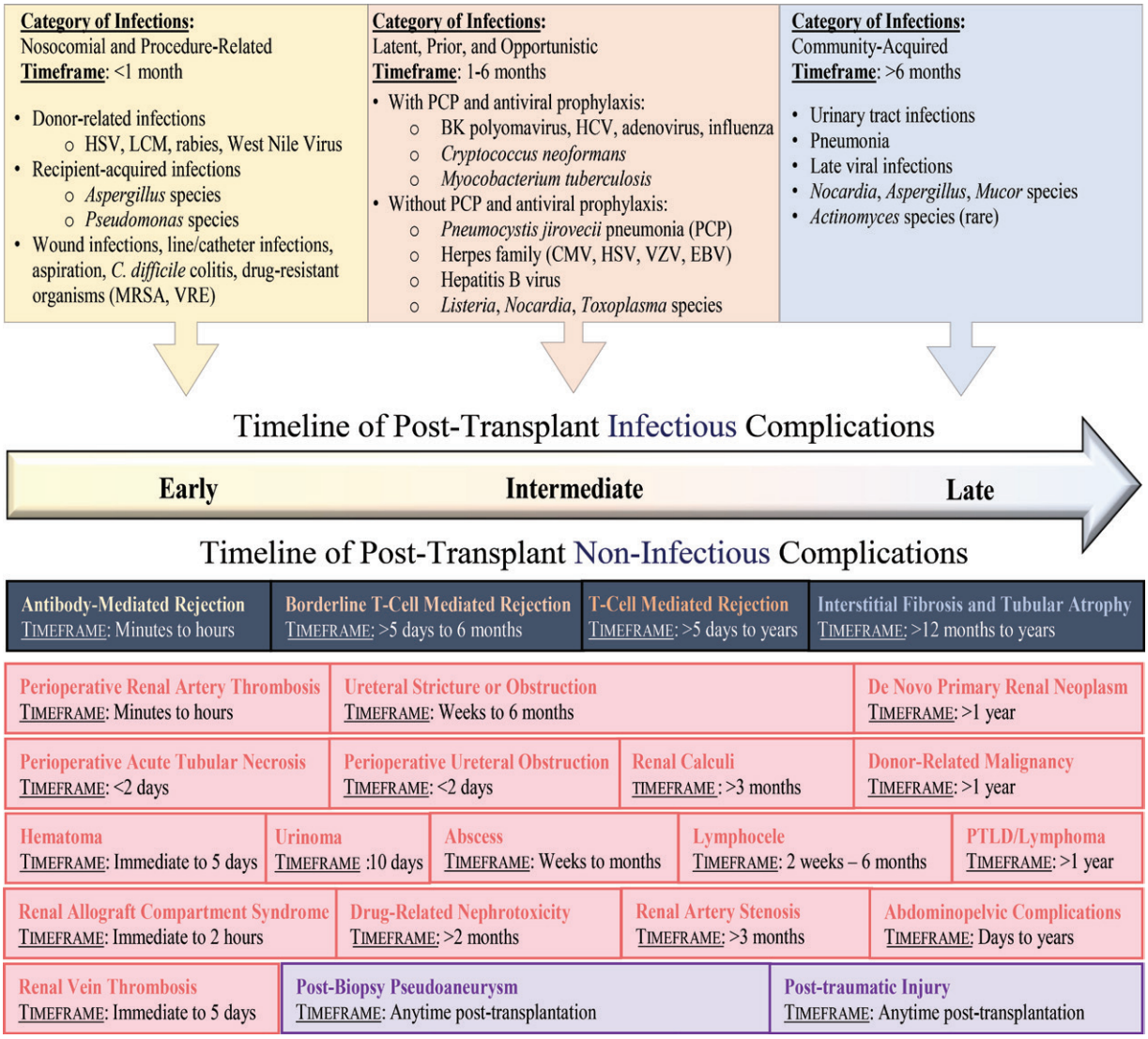

Figure 2. Timeline of renal transplant complications. *C difficile* = *Clostridium difficile*, *CMV* = cytomegalovirus, *EBV* = Epstein-Barr virus, *HCV* = hepatitis C virus, *HSV* = herpes simplex virus, *LCM* = lymphocytic choriomeningitis virus, *MRSA* = methicillin-resistant *Staphylococcus aureus*, *PCP* = *Pneumocystis jirovecii* pneumonia, *PTLD* = posttransplant lymphoproliferative disorder, *VRE* = vancomycin-resistant enterococci, *VZV* = varicella-zoster virus.

occur after renal transplantation (Fig 2) (31). Major categories of complications include perioperative or iatrogenic complications, perinephric fluid collections, vascular complications, urinary complications, generalized abdominopelvic complications, allograft rejection, infections, and malignancies. Each of these major categories is comprised of a variety of posttransplant complications, many of which have well-described clinical and imaging features and a generally predictable time course after transplantation. For example, type of infection can vary on the basis of time from transplantation, with nosocomial and procedure-related infections occurring predominantly in the early period, latent and opportunistic infections occurring in the intermediate period, and community-acquired infections occurring in the late period.

Not all complications occur in isolation: some entities constitute more than one complication category, and conversely, more than one complication can coexist in the same patient. However, the general conceptual framework of categorizing complications with respect to time since transplantation can allow more efficient discrimination between differential considerations during imaging and clinical workup.

Perioperative or Iatrogenic Complications

Routine use of immediate postoperative US in the postanesthesia care unit (PACU) allows rapid diagnosis of surgical and perioperative complications after renal transplantation. Perioperative and iatrogenic complications include those related to surgical technique, anatomic

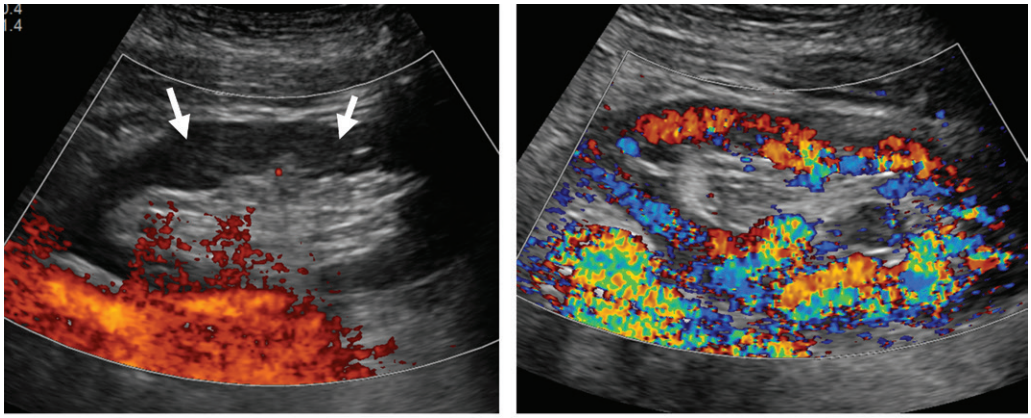

a. b.

Figure 3. Renal allograft compartment syndrome in a 65-year-old woman after deceased donor renal transplant to the left iliac fossa. **(a)** Immediate postoperative power Doppler image of the left iliac fossa transplant kidney shows complete absence of cortical flow (arrows). Immediate reoperation was needed: The patient was returned to the operating room and the allograft was intraperitonealized, given concern for compartment syndrome due to fascial compression. **(b)** Follow-up color Doppler image of the kidney shows robust cortical flow.

constraints in the case of renal allograft compartment syndrome (RACS), and procedure-related complications such as arteriovenous fistula (AVF), pseudoaneurysm, and hemorrhage. Complications related to surgical technique are typically related to the vascular anastomoses and may secondarily lead to thrombosis of the transplant renal artery or vein (32). RACS and vascular thrombosis typically occur in the immediate postoperative period to several days after surgery. Iatrogenic complications related to biopsy can occur after any biopsy performed over the life of the transplant regardless of the time since transplantation.

Renal Allograft Compartment Syndrome

RACS is a rare but also underrecognized cause of early allograft dysfunction or loss, which occurs as a result of intracompartment hypertension and ensuing allograft ischemia and can occur with extraperitoneal/retroperitoneal allograft placement (33). Most renal allografts are placed in the extraperitoneal space, which is confined laterally by the pelvic sidewall, anteriorly by the abdominal wall, and posteromedially by the peritoneum (34). Thus, extraperitoneal placement of the transplant kidney in the iliac fossa potentially predisposes the organ to ischemia due to RACS. This can be the result of direct parenchymal compression related to a mismatch between the extraperitoneal space and the size of the organ or due to extrinsic vascular compression (34). Large width and length of the allograft are characteristics most associated with increased risk for RACS, likely due to lack of compliance in a constrained anatomic compartment (33). Technical causes of RACS related to surgical technique such as non–tension-free or tight fascial closure may potentially be prevented with use of a mesh fascial closure (35).

Extrinsic pressure on the allograft from a perinephric fluid collection such as a postbiopsy hematoma may also occur (36). Since the peritoneum overlying the transplant kidney is usually violated intraoperatively when laparoscopic or robot-assisted transperitoneal placement of the allograft is performed, there is a theoretical risk of hemorrhage extending into the peritoneal cavity through an iatrogenic defect. Thus, while the risk of postbiopsy hemorrhage requiring intervention is low (0.6% in one case series) (37), the threshold for performing follow-up imaging in the setting of clinically suspected bleeding should be relatively low.

In the PACU setting, absent or diffusely diminished cortical flow in the renal allograft at color or power Doppler US suggests the diagnosis of RACS, which usually manifests within 2 hours after transplantation (Fig 3) (34). Immediate recognition of this entity is critical, as the allograft may be salvaged by immediate reoperation. In contrast to RACS, intraperitoneal placement of the renal allograft imparts a greater degree of mobility and thus makes the kidney susceptible to torsion (38).

Postbiopsy Renal AVF and Pseudoaneurysm

Iatrogenic complications related to biopsy can result from biopsies performed before transplantation, intraoperatively, or as part of a posttransplantation protocol and diagnostic procedures. Allograft biopsy can be performed with a 16- or 18-gauge spring-loaded automatic biopsy device, with sampling of the renal cortex using a cortical tangential

RadioGraphics

Figure 4. Postbiopsy pseudoaneurysm and arteriovenous fistula (AVF). **(a)** Color Doppler image shows a round area of bidirectional flow (arrow) in the upper transplant kidney, consistent with a pseudoaneurysm. Spectral analysis at a site of focal aliasing near the pseudoaneurysm shows high-velocity systolic flow and low-resistance diastolic flow, characteristic features of an AVF. **(b)** Three-dimensional volume-rendered image shows the renal artery (white arrow) with an early draining vein (black arrow) as well as the pseudoaneurysm (arrowhead). **(c)** Image from subtraction angiography shows the pseudoaneurysm (arrowhead) and the early draining vein from the AVF (arrow). **(d)** Image from subtraction angiography shows both the pseudoaneurysm and the early draining vein from the AVF treated with coil embolization.

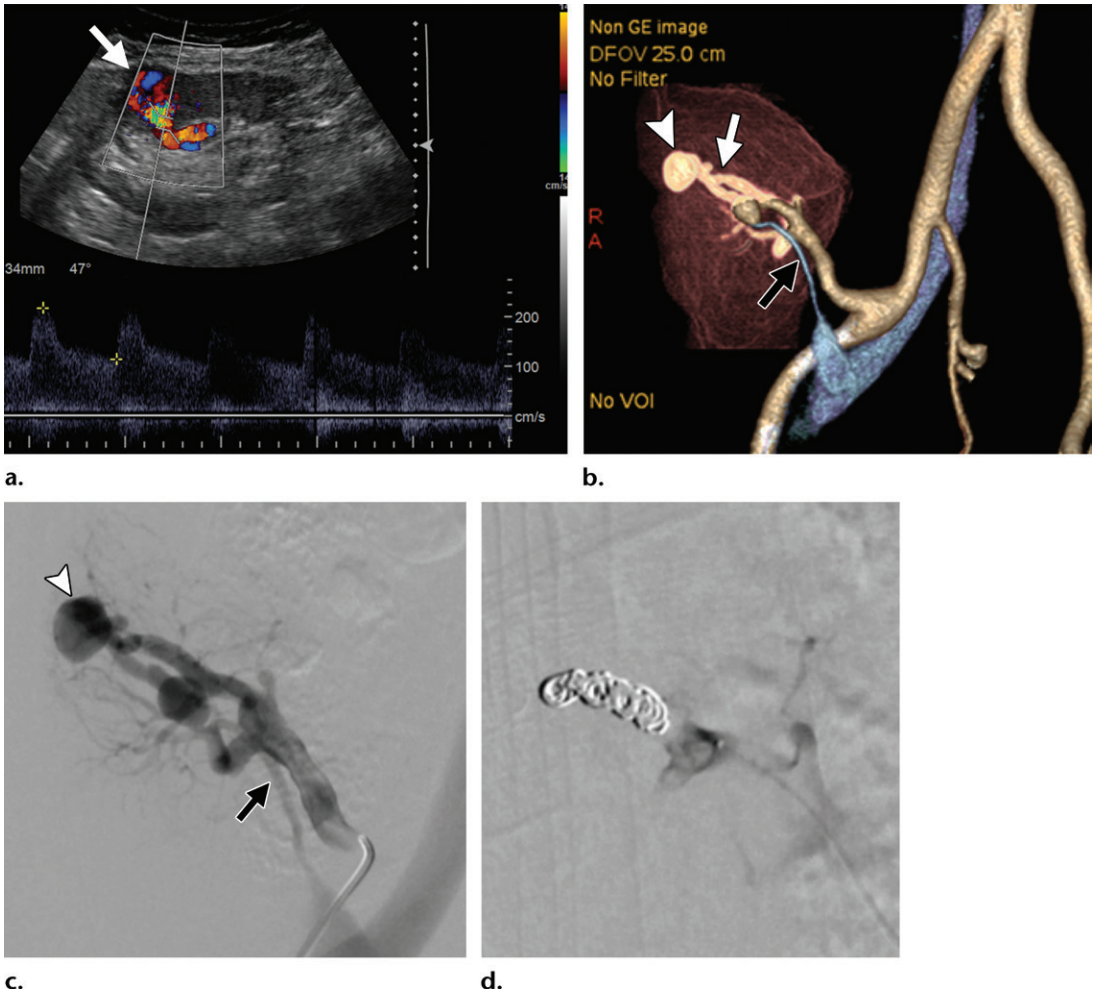

approach (37,39,40). The ideal biopsy specimen is composed entirely of cortical tissue, as samples from the renal medulla generally make little contribution to the histopathologic analysis (41).

Major complications of allograft biopsy are *(a)* those that require transfusion, surgical or vascular intervention, unanticipated hospitalization, or transplant removal and *(b)* death (37). Fortunately, reported rates of these major complications are as low as 0.24% (although reported rates are 0%–4% in the literature) when performed by experienced subspecialist operators, even when supervised trainees are involved (37,41,42).

Minor complications of allograft biopsy include pain, visible hematuria, small perinephric hematoma, and intrarenal AVF (the majority of which are small and hemodynamically insignificant) (40). Gross hematuria after biopsy occurs in 5%–7% of cases and usually resolves spontaneously (22). Need for rebiopsy due to inadequate sampling at initial biopsy (eg, in the case of absence of cortical glomeruli in the obtained specimen) is a technical minor complication that can occur.

It is important to distinguish between a small hemodynamically insignificant postprocedure AVF and a pseudoaneurysm (Fig 4). At color Doppler assessment, both AVFs and pseudoaneurysms can appear as focal areas with disorganized blood flow extending beyond the margins of the normal vessel (22). AVFs have a feeding artery with a high-velocity low-resistance waveform at spectral analysis. The region of disorganized flow is associated with a segmental or interlobar artery with high-velocity turbulent flow, paired with a vein that exhibits aliasing at color Doppler assessment and an arterialized waveform at spectral analysis (22).

Sonographically visible postprocedure AVFs have been reported in up to 10% of renal allograft biopsies, most of which are asymptomatic with no clinically significant hemodynamic consequences. These cases can be treated conservatively and can be followed up with US as needed, with 70% regressing or resolving spontaneously (40,43). Large or symptomatic AVFs resulting in abnormal large or persistent gross hematuria or significant hypertension occur in only 1%–2% of cases and can be treated with catheter embolization (40). Transcatheter embolization in these cases has been shown to be an effective therapy, with relatively low rates of long-term detrimental effects on the allograft, and may lead to improved renal function and resolution of hematuria (44).

In counterdistinction, a pseudoaneurysm is a contained vascular bleed or leak from an intraparenchymal artery due to injury to all three layers of the arterial wall. It may require intervention, particularly if large (historically >2 cm) or progressively growing in size (22).

At gray-scale US, an intrarenal pseudoaneurysm may appear as a mildly complex cystic structure but can also mimic a simple renal cyst. Thus, color or power Doppler assessment must be used for all anechoic cystic-appearing structures identified at gray-scale US. Classic color Doppler findings of postbiopsy pseudoaneurysm, particularly those with a narrow neck, include a to-and-fro pattern of blood flow within the neck and the yin-yang sign of swirling blood within the sac (Fig 4) (22,45).

Contrast-enhanced CT angiography plays an important role in delineating the anatomy of an AVF or better characterizing a pseudoaneurysm if endovascular intervention is planned. Nonenhanced MR angiography with steady-state free precession (SSFP) sequences may also be a useful adjunct for vascular mapping when gadolinium contrast material cannot be administered owing to renal insufficiency (46). Contrast-enhanced T1-weighted MRI shows a contrast material–filled intraparenchymal vascular lesion that may be ovoid, lobulated, or irregular near the site of biopsy. Nonenhanced T1- and T2-weighted MR images may show subcapsular hematoma or uncontained hemorrhage with layering dependent blood products (Fig 5). Contrast-enhanced US is a relatively new tool for evaluating vascular anatomy and can be used if available.

Overall, transplant kidney biopsy using a tangential cortical technique is a safe procedure in which the benefits usually outweigh the risks. Consensus guidelines for classifying rejection allow histopathology-based diagnosis and appropriate therapy and warrant biopsy in many cases. Knowledge of the complications of allograft biopsy and their imaging appearances—particularly at US, the usual first-line imaging tool—is pivotal in quickly and effectively managing the rare serious complications that can occur.

Perinephric Fluid Collections

There are four main types of perinephric fluid collections commonly encountered in the renal transplant recipient: hematoma, urinoma, abscess, and lymphocele, occurring roughly chronologically in that order with respect to time from surgery (Table) (22). Imaging features at gray-scale US may overlap; however, differentiation can often be achieved with use of color Doppler US and in conjunction with ancillary clinical information. Time from surgery is a key consideration in discriminating between these types of fluid collections in conjunction with clinical manifestations and imaging findings.

When large, perinephric fluid collections can exert mass effect on the transplanted kidney. Mass effect is more likely to develop in the confined extraperitoneal space, where most allografts are located, as compared with the intraperitoneal compartment (47). When differentiation between perinephric fluid collections will influence treatment plans, diagnostic aspiration and fluid analysis may be performed.

Perinephric Hematoma

In the immediate postoperative period, perinephric hematomas are common and should be documented during postoperative baseline US. While hematomas resolve spontaneously, a small minority may require surgical evacuation, usually in the setting of significant mass effect on the transplant kidney or continuous hemorrhage warranting transfusion (48).

At US, peritransplant blood products can appear anechoic, hypoechoic, or hyperechoic, depending on the degree of blood product evolution. Hyperacute blood products in the setting of active bleeding can appear anechoic, but usually there will be areas with echogenic mobile debris, signifying complexity (49). Acute hematoma can appear heterogeneously hyperechoic, with subsequent development of heterogeneous central hypoechoic or cystlike areas with scattered internal thin septa in the late state, indicating clot lysis as the hematoma evolves over time (49,50). With gray-scale US alone, clinically significant perinephric hematomas may be underdiagnosed and their volume may be underestimated; thus, correlation with hemoglobin levels may be useful (51). At nonenhanced CT, acute hematomas are hyperattenuating collections (>30 HU), and at MRI, they typically have

RadioGraphics

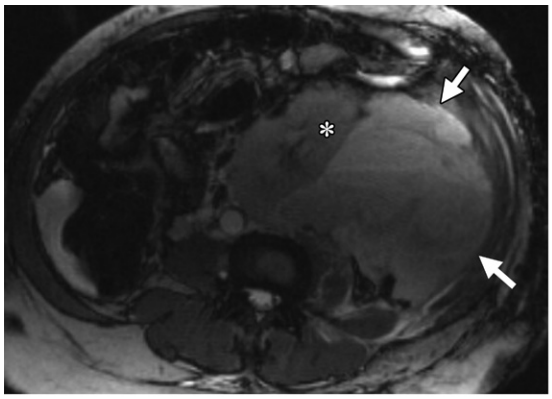

a.

b.

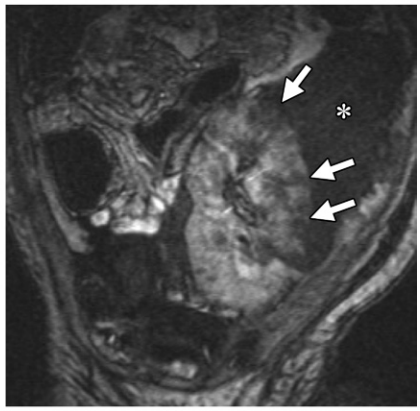

c.

Figure 5. Postbiopsy pseudoaneurysm with subcapsular hematoma and uncontained hemorrhage in a 58-year-old patient after recent tissue sampling. **(a)** Axial balanced steady-state free precession (SSFP) MR image shows a left iliac fossa renal transplant (*) with a large perinephric hematoma (arrows), which causes mass effect on the allograft. Note the internal heterogeneity and layering material, compatible with evolving blood products. **(b)** Coronal MIP MR angiogram shows a saccular contrast material–filled vascular abnormality (arrow) within the renal transplant, compatible with a postbiopsy pseudoaneurysm. **(c)** Coronal contrast-enhanced T1-weighted MR image shows heterogeneous enhancement of the renal transplant (arrows). Note the large nonenhancing perirenal fluid collection (*).

Transplant Kidney Periallograft Fluid Collections

Fluid Collection	Time Frame	Imaging Features	Results of Fluid Analysis
Hematoma	Immediately after surgery to 5 d	Complex heterogeneous collection with internal septa and retracting clot Hyperattenuating components at nonenhanced CT	Not usually aspirated owing to risk of superinfection
Abscess	Weeks to months	Peripheral enhancement at contrast-enhanced CT Increased peripheral blood flow at Doppler US Thickened wall	Purulent material Numerous PMNs
Urinoma	10 d	Simple collection with fluid attenuation Contrast material extravasation at delayed contrast-enhanced CT Extraurinary tracer excretion at renal scintigraphy (eg, ^{99m}Tc-MAG$_3$ or ^{99m}Tc-DTPA)	Fluid Cr > serum Cr Fluid K^+ > serum K^+
Lymphocele	2 w to 6 mo	Fluid-attenuation collection lacking epithelial lining With or without thin internal septa, often adjacent to allograft or along pelvic sidewall	Fluid Cr ≈ serum Cr Fluid K^+ ≈ serum K^+

Note.—Cr = creatinine concentration, DTPA = diethylenetriaminepentaacetic acid, K^+ = potassium concentration, PMN = polymorphonucleocyte.

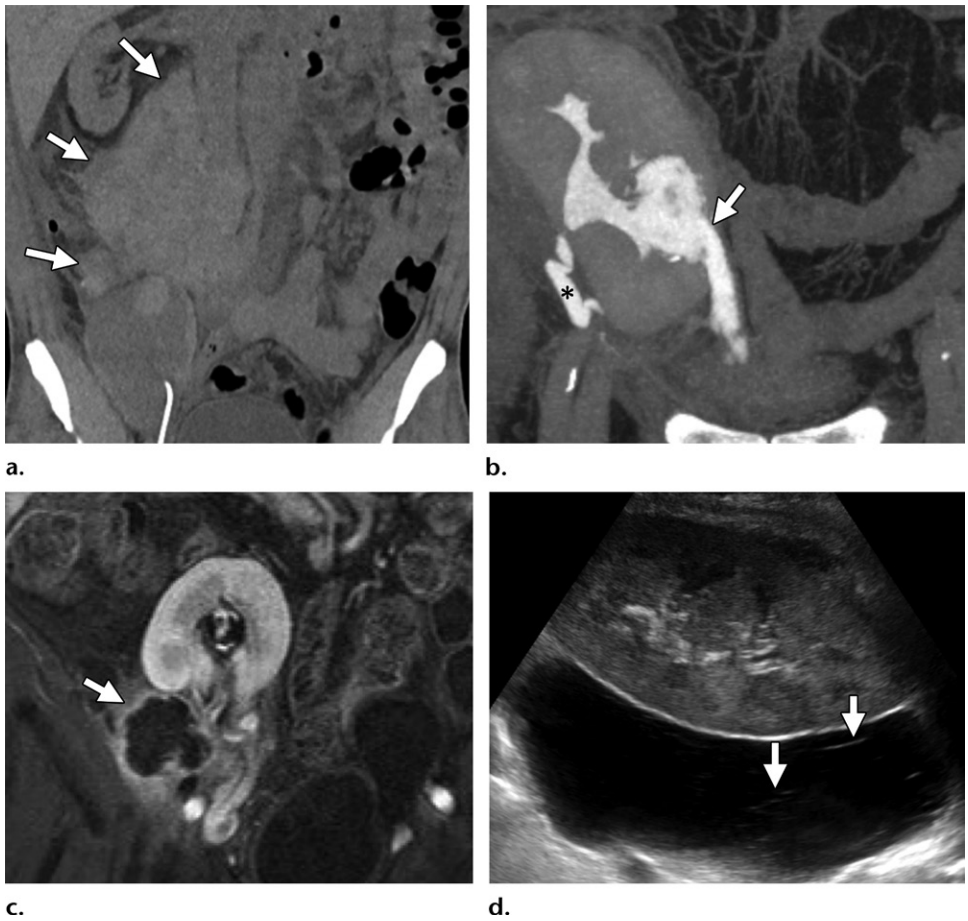

Figure 6. Four types of perinephric fluid collections. **(a)** Coronal nonenhanced CT image shows a hyperattenuating perinephric hematoma (arrows). **(b)** Coronal contrast-enhanced delayed phase MIP CT image shows focal urinary contrast material leak from the collecting system (arrow), which resulted in a dependent perinephric urinoma (not shown). Note the contrast material–filled transplant ureter (*). **(c)** Coronal gadolinium-enhanced T1-weighted MR image shows a peripherally enhancing thick-walled abscess (arrow). **(d)** Gray-scale US image shows a hypoechoic collection with thin echogenic septa (arrows), in this case without mass effect. Aspiration of the collection showed a creatinine concentration similar to that of serum levels, consistent with lymphocele.

intrinsic increased signal intensity on precontrast T1-weighted images (Fig 6a).

Differentiation between perirenal and subcapsular collections is important. A subcapsular collection is more likely to cause mass effect on the renal parenchyma and is usually crescentic, with extension along the contour of the kidney deep to the renal capsule (52).

It is important to consider that posttraumatic perinephric hematoma can occur at any time after transplantation. Extraperitoneally placed allografts in the lower abdomen are not protected by the ribs from blunt trauma, as is the case for the native kidneys (Fig 7).

Urinoma

A urinoma is a fluid collection that has leaked from the renal collecting system (usually the renal pelvis), ureter, or ureteroneocystostomy site and is usually found in the first 10 days after transplantation, most commonly interposed between the allograft and the urinary bladder (22,34,53,54). Urinomas usually occur in the setting of inadequate blood supply to the ureter or elevated pressures from obstruction (22). Caliceal or forniceal leakage is less common but can occur (22).

The US appearance of urinoma may overlap with that of lymphocele or seroma, appearing as a simple hypoechoic fluid collection. Further diagnostic workup may include delayed contrast-enhanced CT or MRI to assess the collecting system and ureteral anastomoses and detect leakage of excreted contrast material (Fig 6b). Retrograde urography or renal scintigraphy can also be performed. Radionuclide scintigraphy using ^{99m}Tc MAG_3 shows progressive extraurinary accumulation of radiopharmaceutical in an area that is initially photopenic and may demonstrate mass effect by the perinephric collection on the transplant kidney (Fig 8) (55).

Fluid aspirated from a urinoma will have creatinine and potassium concentrations greater

RadioGraphics

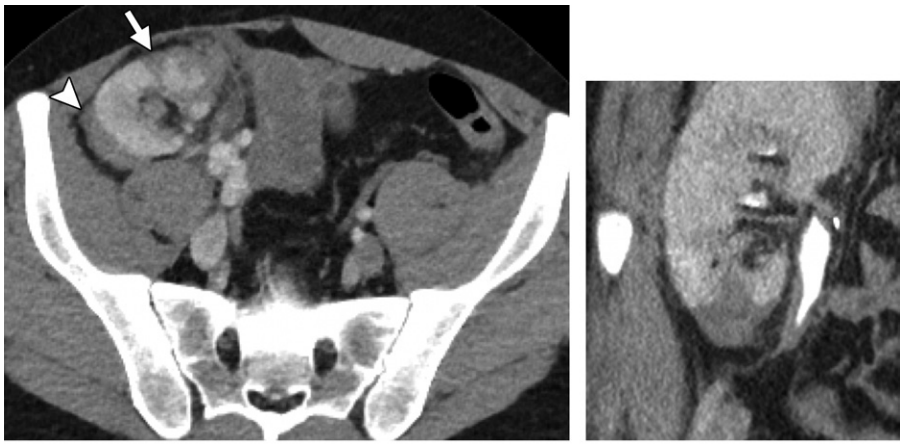

a. b.

Figure 7. Traumatic AAST (American Association for the Surgery of Trauma) grade 3 injury of a renal allograft in a 46-year-old patient with posttraumatic renal transplant laceration after a motor vehicle collision. **(a)** Axial contrast-enhanced CT image shows a right iliac fossa renal allograft with irregular hypoattenuating lacerations through the parenchyma (arrow), which measure greater than 1 cm in depth, as well as a small high-attenuation perinephric hematoma (arrowhead). **(b)** Coronal contrast-enhanced CT image during the excretory phase shows no contrast material leak to suggest involvement of the collecting system, consistent with an AAST grade 3 renal injury.

than those in the blood serum, whereas the more commonly encountered lymphocele aspirate will yield creatinine and potassium concentrations comparable to serologic concentrations (56). Identification of urinoma is important even in the absence of mass effect, as these fluid collections may result in electrolyte imbalances or can become superinfected (56).

Perinephric Abscess

Infected perinephric fluid collections usually develop within the first weeks to months after transplantation (53,57). Abscess formation in the perinephric space may manifest as a complication of renal allograft infection or infection of adjacent abdominopelvic organs or through local spread of an abdominal wall infection. Fever and leukocytosis in conjunction with a perinephric fluid collection should raise suspicion for superimposed infection. Perirenal abscess can appear as an irregular thick-walled fluid collection with peripheral hyperemia and surrounding inflammatory change in the peritransplant fat (Fig 6c).

At US, these collections typically are heterogeneously hypoechoic with internal debris and septa, with blood flow present in the thickened wall and septa at color Doppler assessment. CT and MRI are valuable for evaluating disease extent and detecting involvement of adjacent structures. Since the iliac fossa is the most common location for allograft transplantation, perinephric abscesses may involve the adjacent psoas muscle or adnexal structures in female patients. Prompt treatment with systemic antibiotics plus percutaneous drainage or surgical management is important given the immunosuppressed status of these patients (54).

Lymphocele

Lymphocele is the most commonly encountered perinephric fluid collection, typically occurring 2 weeks to 6 months after surgery, and is the most common collection resulting in allograft hydronephrosis (22,58). These fluid collections, which lack a true epithelial lining at histologic analysis, occur along the lymphatic drainage pathways in the postoperative patient and are often asymptomatic (58). At US, these collections are characteristically well marginated and anechoic, occasionally containing thin internal septa (Fig 6d). Lymphoceles are characterized by a barely perceptible wall and internal simple fluid attenuation at CT and high T2 signal intensity at MRI.

Infrequently, these lymph-filled collections cause mass effect on the transplant kidney, ureter, vasculature, or urinary bladder, in which case US-guided percutaneous drainage or laparoscopic peritoneal fenestration may be performed (59,60). Percutaneous catheter drainage results in high rates of reaccumulation (approaching 90%); thus, sclerosing agents such as ethanol, povidone-iodine, or fibrin glue have been used as alternatives with varying degrees of success (57). Although nonspecific, lymphoceles can be associated with allograft rejection and are thought to be the result of increased regional lymph flow in the setting of inflammation (58).

Figure 8. Perinephric urinoma diagnosed with renal scintigraphy in a 53-year-old woman after living donor renal transplant with delayed graft function requiring hemodialysis. On postoperative day 13, she developed fullness over the transplant kidney. **(a)** Gray-scale US image shows a nonspecific perinephric fluid collection (arrows). **(b)** ^{99m}Tc MAG_3 renal scintigram shows prompt radiopharmaceutical uptake in the allograft (*) and subsequent excretion into the urinary bladder (arrowhead). **(c)** Right lateral *(RT LAT)* and anterior *(ANT)* delayed static images show ill-defined radiopharmaceutical accumulation anterior and lateral to the transplant kidney, compatible with a urinoma, which was confirmed at surgery.

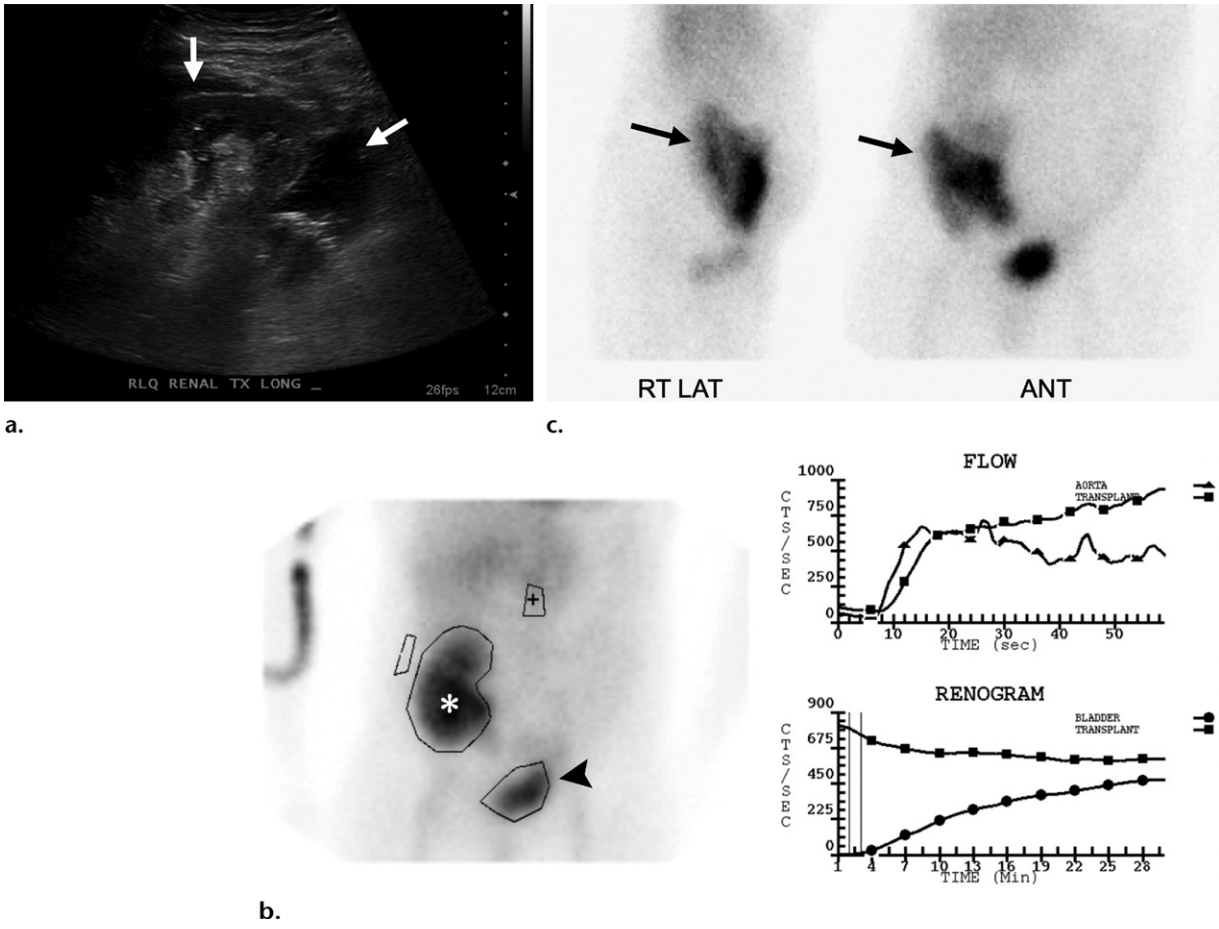

Vascular Complications

Vascular complications may occur at any time after transplantation but are particularly important in the early postoperative period, as correction of acute vascular thrombosis may allow salvage of the allograft. Thrombosis of the transplant renal artery or vein may occur immediately after surgery or as late as 5 days postoperatively. Renal artery stenosis is usually seen 3 months or later after surgery, as its causes tend to be multifactorial.

Renal Artery Thrombosis

Renal artery thrombosis is a rare but serious complication, with prevalence of approximately 0.4%, but when present can result in graft loss (61,62). It most often develops in the early postoperative period (within minutes to hours) and can occur as a result of hyperacute rejection, anastomotic occlusion, kinking of the renal artery, or presence of an intimal flap (22). Vasculitis and external compression of the renal artery, such as in the setting of prolonged decubitus patient positioning, have been identified as rare causes of renal artery thrombosis with case reports in the literature (22,63). A very rare reported cause of late renal artery thrombosis is external renal artery compression related to left lateral decubitus patient positioning during right total hip arthroplasty, approximately 12 months after renal transplantation (64).

Clinical signs of renal artery thrombosis include abrupt cessation of urine output and worsening hypertension (22,61). Although the graft is denervated, pain in the general location of the graft may manifest as a result of peritoneal irritation secondary to graft infarction and associated swelling and inflammation along the margin of the peritoneum (22).

Renal infarction can be segmental or global. At US, a segmental infarct appears as a hypoechoic masslike region, which can be ill defined or have a well-defined echogenic wall at gray-scale US, with a corresponding wedge-shaped region of avascu-

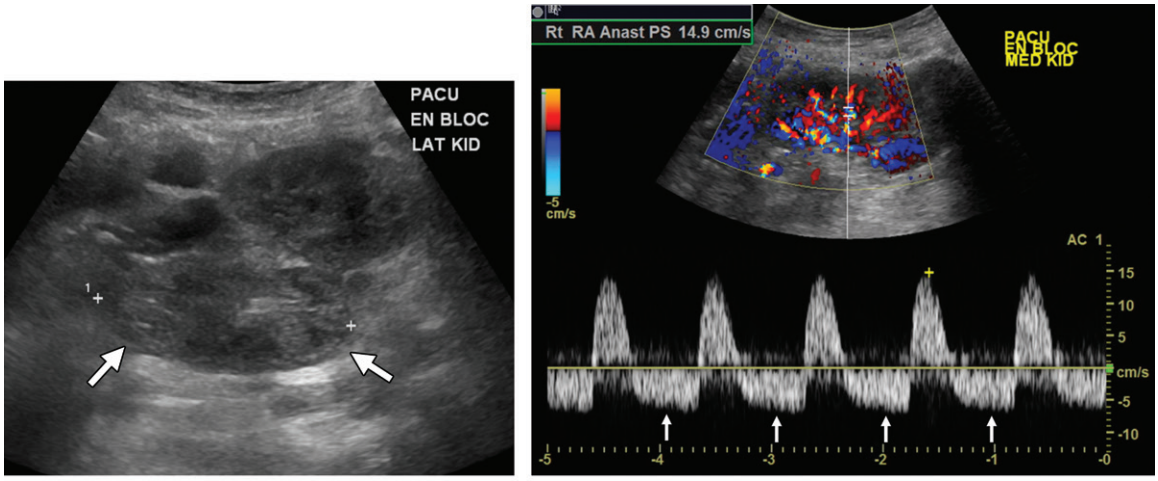

a. b.

Figure 9. Perioperative renal vein thrombosis after transplantation of pediatric en bloc kidneys. **(a)** Gray-scale US image of en bloc pediatric kidneys shows heterogeneity of the lateral renal moiety (arrows). **(b)** Color Doppler image with spectral tracing of the intrarenal artery in the medial renal moiety shows classic reversed diastolic flow (arrows) with preserved systolic arterial upstroke, highly concerning for renal vein thrombosis, which was proved at allograft nephrectomy.

larity at color or power Doppler assessment. Correlation with symptoms and urinalysis results is important, as these findings can also be seen with pyelonephritis or transplant kidney rupture (22).

In the case of global infarct, which can occur with total vascular obstruction, absence of blood flow will occur throughout the graft at color and power Doppler US. Early accurate diagnosis is critical, as immediate intervention is required for graft salvage (22). In situations where there is not a clinical indication for immediate surgical reexploration and US results are nondiagnostic, MR angiography, digital subtraction angiography (DSA), or renal scintigraphy may be performed (65). MR angiography or DSA will show diminished or absent flow to the allograft and an abrupt cutoff in the transplant renal artery (66). At renal scintigraphy, reduced or absent graft perfusion on the time-activity curve will be present, although nonspecific for thrombosis, as this can also be seen with rejection (67).

Renal Vein Thrombosis

Renal vein thrombosis is reported to occur in less than 5% of adult patients and up to 8.2% of pediatric patients, but accounts for early graft failure in up to 8% of adult patients and up to 35% of pediatric patients (22,28,61,65,68). It usually occurs within the first 5 days after surgery, with peak incidence within the first 48 hours, although there are cases of delayed renal vein thrombosis occurring after the 1st postoperative week (22,65).

Donor risk factors associated with thrombosis include donor age less than 6 years or greater than 60 years, allograft cold ischemia time greater than 24 hours, renal artery atherosclerosis, and right-sided allograft (28). Recipient risk factors associated with thrombosis include recipient age less than 6 years or greater than 50 years, exclusive peritoneal dialysis, hypercoagulable states, atherosclerosis, diabetes mellitus, and technical surgical complications (28). Hypovolemia, multiplicity of renal veins, and discrepancies in blood vessel size between donor and recipient have also been implicated (69).

Early findings of renal vein thrombosis at US include edematous engorgement of the kidney, loss of corticomedullary differentiation, and perinephric fluid (Fig 9a). Reversed diastolic flow in the transplant renal artery at spectral Doppler US is highly suggestive of renal vein thrombosis (Fig 9b) but may also be seen less frequently with disorders such as allograft torsion, severe allograft rejection, or acute tubular necrosis (ATN) (70). When reversed diastolic flow in the transplant artery is identified, the renal vein should be carefully interrogated to assess for renal vein thrombosis.

Early accurate diagnosis is critical for graft salvage, which has been reported even up to 15–20 hours after onset of symptoms, which include rapid onset of pain, oliguria or anuria, and thrombosed veins in the ipsilateral thigh (28,71). Open surgical thrombectomy is usually performed to reestablish venous outflow. In the case of late renal vein thrombosis, endovascular thrombolysis may be considered but carries greater risk of bleeding (28). In addition to US, diffusion-weighted MRI may be used to monitor perfusion changes in the allograft after renal vein thrombectomy (72).

Transplant Renal Artery Stenosis

The most common vascular complication of renal transplantation is renal artery stenosis,

Figure 10. Renal artery stenosis after deceased donor renal transplant 2 years earlier in a 33-year-old woman with a history of lupus nephritis. **(a)** Color Doppler US image of the proximal renal artery shows elevated peak systolic velocity of 575 cm/sec. **(b)** Intrarenal arterial spectral tracing shows a classic tardus-parvus waveform distal to the arterial stenosis. **(c)** Coronal gadolinium-enhanced MIP T1-weighted MR image shows high-grade stenosis of the transplant renal artery at the anastomosis (arrow). **(d)** Angiogram after balloon angioplasty shows the artery as widely patent (arrow).

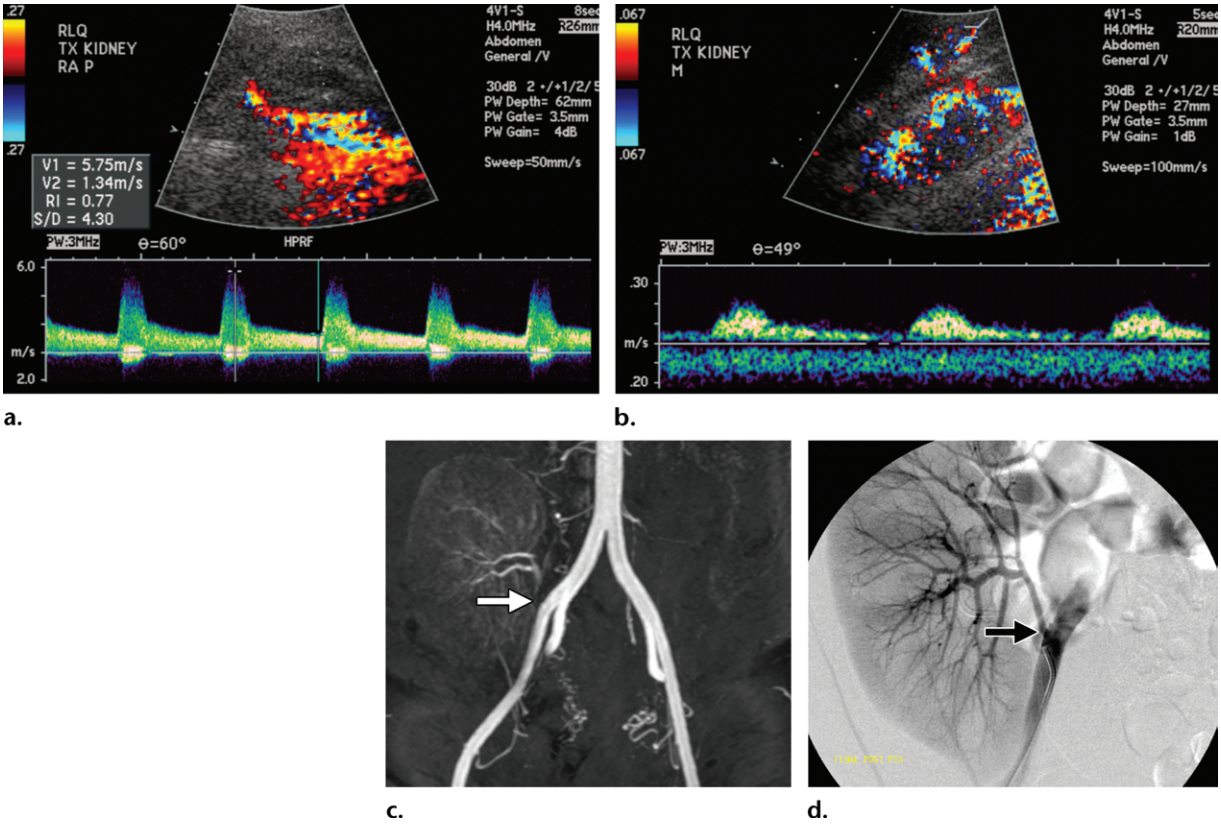

affecting about 3% of all renal transplants and typically manifesting 3 months to 2 years after transplantation (73–75). Arterial hypertension refractory to treatment is the most common clinical scenario, occurring in 93% of cases, often as a single event (53%) or combined with a decline in renal function (44%) (74).

Direct signs of transplant renal artery stenosis are seen at the site of narrowing and include elevated peak systolic velocity (PSV), abnormal ratio of PSV in the main renal artery with respect to the upstream iliac artery, and presence of aliasing due to turbulence (25). Historically, PSV exceeding 250 cm/sec in the transplant main renal artery or ratio of main renal artery PSV to ipsilateral external iliac artery (EIA) PSV (measured proximal to the anastomosis) greater than 1.8 has been used to suggest significant transplant renal artery stenosis. Recent data suggest that this upper threshold value of 250 cm/sec for PSV and use of a ratio of 1.8 for main renal artery PSV to EIA PSV may lead to false-positive diagnoses of renal artery stenosis. A 2017 study (75) found that 26% of patients without renal artery stenosis had main renal artery PSV greater than 250 cm/sec within the first 9 months after transplantation. Within 1 year of transplantation, 18% of patients without renal artery stenosis had main renal artery PSV greater than 250 cm/sec (75).

In the absence of other signs or changes to the arterial waveform, an absolute PSV of 340–400 cm/sec at the anastomosis has been suggested as a more reliable cutoff for transplant renal artery stenosis (Fig 10a) (75). Indirect signs of renal artery stenosis are seen distal or downstream to the site of stenosis, in the main renal artery or end-organ arteries, and include delayed or blunted systolic upstroke at spectral analysis (tardus-parvus waveform) (Fig 10b). Relatively reduced RIs may also be seen (25).

In the perioperative period, isolated elevated PSV in the renal artery may be related to postoperative edema or technical challenges of the examination. Short-term follow-up Doppler US may be performed to reassess the renal artery, although studies have shown that the PSV may gradually decrease over the course of months, not days (76,77). Therefore, main renal artery PSV should be considered in context along with spectral waveforms of the transplant artery, intraparenchymal arterial RIs, patency of venous outflow, and patient risk factors (78).

RadioGraphics

When suspicion for transplant renal artery stenosis is high on the basis of findings at duplex US, further evaluation with MR angiography, carbon dioxide angiography, or angiography with iodinated contrast material may be performed (Fig 10c). Carbon dioxide angiography is a useful tool for transplant recipients, as it allows both diagnostic evaluation and therapeutic intervention while reducing the required volume of iodinated contrast material (79). When transplant renal artery stenosis is hemodynamically significant, endovascular techniques including percutaneous transluminal angioplasty and stent placement are first-line treatments, followed by surgery in refractory cases or in the setting of complex arterial anatomy (Fig 10d) (73).

Obstructive Urologic Complications

The incidence of ureteral complications has decreased significantly in recent years owing to improvements in harvesting techniques that better preserve ureteral perfusion, use of shorter ureters, and decrease in average steroid use (80). Ureteral obstruction has a bimodal distribution, uncommonly occurring in the first 1–2 days after surgery and more often occurring beyond the 1st postoperative month, typically within the first 6 months, with a prevalence of 2%–7.5% and is usually the result of ureteral stenosis (80). These cases can be due to ischemia or scar tissue leading to ureteral stricture, extrinsic compression from an abscess or lymphocele, or less commonly intraluminal abnormalities such as stone disease (80).

Renal transplant patients are at increased risk for urolithiasis compared with the general population, but only 1%–2% develop clinically significant stones (22). Early ureteral obstruction is uncommon and usually related to ureteral kinking, ischemia, or external compression from postoperative edema or hematoma in the perioperative period (80,81). A ureteral stent is commonly placed at the time of surgery to reduce the risk of early ureteral obstruction.

Allograft dysfunction secondary to transplant ureteral obstruction manifests as diminished renal function with elevated serum creatinine level and presence of hydronephrosis at imaging, usually at US (80). Evaluation for ureteral obstruction at US should include assessment of the collecting system and transplant ureter from the level of the hilum to the urinary bladder, noting the presence of any periureteral fluid collections producing mass effect or the presence of intraluminal debris or stones. Whenever new hydronephrosis is identified, correlation with results of urinalysis and physical examination should be performed to exclude superimposed infection such as pyonephrosis, which can appear identical to hydronephrosis and is an emergency requiring rapid intervention. However, in most cases of pyonephrosis, urothelial thickening and layering debris will be present within the dilated renal collecting system, ureter, and urinary bladder (50).

In the absence of allograft dysfunction and secondary features of obstruction, it may be within acceptable limits to observe mild pelvicaliectasis due to the dependent orientation of the allograft in the iliac fossa and an increased tendency for vesicoureteral reflux (81). The increased tendency for vesicoureteral reflux is due to the relatively shorter length of the transplant ureter and loss of the normal obliquity and submucosal tunnel within the urinary bladder after ureteroneocystostomy (81,82).

Transplant ureteral stenosis is typically managed endoscopically with retrograde balloon angioplasty and stent placement (83). Stricture excision with ureteral reimplantation can be performed for distal lesions if there is adequate ureteral length. When scarring or granulation tissue is exuberant or obstructs the ureteropelvic junction (UPJ), more creative approaches may be required, such as donor-to-native ureteroureterostomy or pyelovesicostomy, in which an anastomosis is created directly between the transplant renal pelvis and recipient bladder (Fig 11) (84).

Abdominopelvic Complications

A number of postoperative complications may arise in the vicinity of the allograft or as a result of renal transplantation. Laparoscopic and robot-assisted transplant surgical techniques involve extraperitonealization of the allograft via a peritoneal window. Thus, these patients are susceptible to the same postoperative complications experienced by other surgical patients in whom the peritoneum has been violated.

These include but are not limited to fascial dehiscence and bowel or allograft evisceration, which tend to occur in the perioperative period, and small bowel obstruction (Fig 12), which usually manifests after the first few months to years after surgery (85–87). Bowel obstruction with or without closed-loop physiology can occur as a result of adhesive disease. It can appear at CT as fluid-filled dilated loops of small bowel with a single or multiple transition points, depending on the extent of adhesive disease and the presence of mesenteric edema (88).

The relatively superficial position of the transplant kidney in the iliac fossa makes it particularly susceptible to both blunt and penetrating trauma, which can occur at any time after transplantation (Fig 7). Whereas the native kidneys are protected by retroperitoneal fat, musculature,

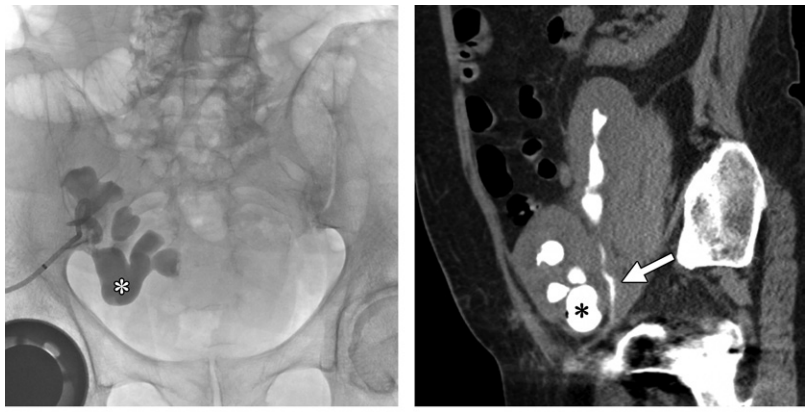

a. b.

Figure 11. Ureteropelvic junction (UPJ) obstruction due to desmoplastic reaction, scar tissue, and kinking at the UPJ of the lower moiety in a patient with en bloc adult deceased donor kidney transplant in the right lower quadrant. **(a)** Fluoroscopic image obtained during antegrade pyelography of the lower transplant kidney shows severe pelvicaliectasis (*) without opacification of the urinary bladder, consistent with UPJ obstruction. **(b)** Subsequent sagittal nonenhanced CT image after antegrade injection of contrast material into the collecting systems shows persistent pelvicaliectasis of the lower moiety (*) and visualization of only the normal-caliber upper moiety transplant ureter (arrow). Pyelovesicostomy of the inferior allograft with bladder flap and hitch was performed (not shown), with resolution of the hydronephrosis.

and ribs, the extraperitoneal space within the lower abdomen housing the allograft lacks these same protective barriers. Nevertheless, principles for evaluation of renal trauma remain the same for both native and transplant kidneys.

CT is the modality of choice for evaluating the extent of traumatic injury. Renal angiography and retrograde pyelography may be used as adjuncts for suspected vascular injuries and ureteral or UPJ injuries, respectively (89). Traumatic injuries can be graded on a scale from 1 to 5 according to the AAST (American Association for the Surgery of Trauma) injury scale, which ranges from mild contusion-related hematuria (grade 1) to avulsion of the renal hilum with associated devascularization (grade 5) (90).

Renal Allograft Parenchymal Complications

Complications intrinsic to the renal allograft parenchyma in the posttransplant period include delayed graft function, allograft rejection, acute tubular necrosis (ATN), and drug-related nephrotoxic effects. The key role of imaging in these cases is to exclude other causes—such as vascular or collecting system abnormalities—that can produce renal transplant dysfunction (91).

Delayed Graft Function

Delayed graft function is defined as the need for dialysis in the 1st week after renal transplantation (92). The greatest risk factor for delayed graft function is cold ischemia time. Other associated factors include infarction, ATN, rejection, and presence of a peritransplant fluid collection (93). The duration of cold ischemia has been shown to be the predominant risk factor for delayed graft function (93).

At gray-scale US, the allograft parenchyma can appear normal. Doppler assessment may reveal absent or diminished diastolic blood flow with elevated RIs, which are nonspecific findings that may also be present in the setting of allograft rejection (91).

Renal Allograft Rejection

The Banff Classification of Allograft Pathology provides a framework for classification of renal allograft rejection based on a combination of histopathologic features coupled with molecular, serologic, and clinical parameters (94). Briefly, Banff lesions describe typical findings of rejection at histologic analysis; a diagnostic category is then assigned, depending on the presence or absence of adjunct findings such as acute thrombotic microangiopathy, increased expression of validated gene transcripts, or arterial intimal fibrosis. The six diagnostic categories are *(a)* normal biopsy results or nonspecific changes, *(b)* antibody-mediated changes, *(c)* borderline changes suspicious for acute T-cell mediated rejection (TCMR), *(d)* TCMR, *(e)* interstitial fibrosis and tubular atrophy (IFTA), and *(f)* other changes not considered to be caused by acute or chronic rejection (94). Antibody-mediated rejection (AMR) is further subdivided into active, chronic active, and chronic forms, whereas TCMR is subdivided into acute and chronic active forms.

RadioGraphics

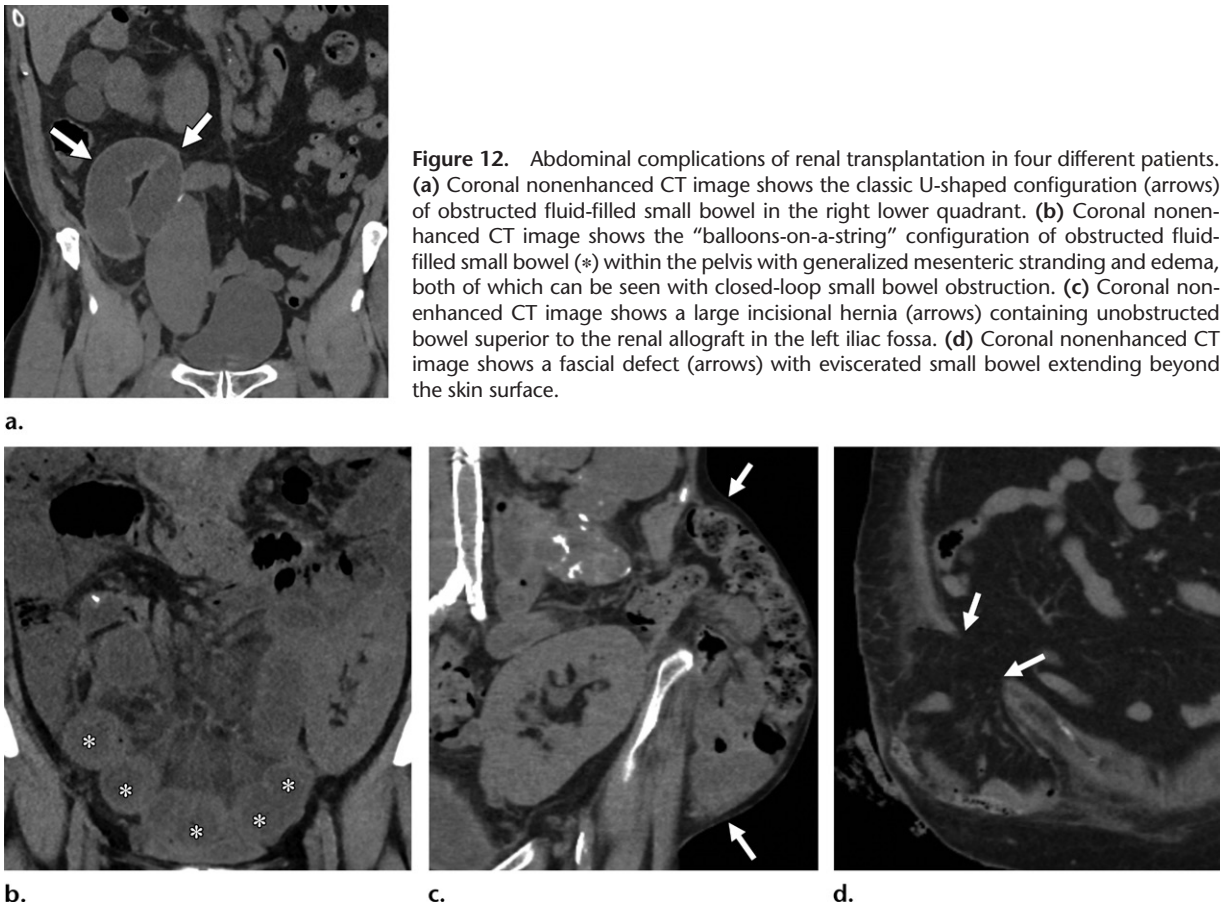

Figure 12. Abdominal complications of renal transplantation in four different patients. **(a)** Coronal nonenhanced CT image shows the classic U-shaped configuration (arrows) of obstructed fluid-filled small bowel in the right lower quadrant. **(b)** Coronal nonenhanced CT image shows the "balloons-on-a-string" configuration of obstructed fluid-filled small bowel (*) within the pelvis with generalized mesenteric stranding and edema, both of which can be seen with closed-loop small bowel obstruction. **(c)** Coronal nonenhanced CT image shows a large incisional hernia (arrows) containing unobstructed bowel superior to the renal allograft in the left iliac fossa. **(d)** Coronal nonenhanced CT image shows a fascial defect (arrows) with eviscerated small bowel extending beyond the skin surface.

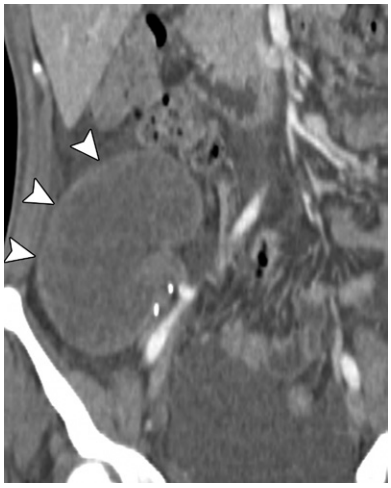

Figure 13. Complete renal allograft infarction due to rejection-related vascular thrombosis 7 years after transplantation. Coronal contrast-enhanced CT image shows diffuse enlargement and nonenhancement of the right lower quadrant transplant kidney, with the "cortical rim sign" of thin capsular enhancement (arrowheads), a feature of infarction.

Before development of the Banff Classification in 1991, rejection was broadly divided into hyperacute, acute, accelerated acute, and chronic rejection phases based on time from transplantation (95). Although the refined classification retains some temporal correlation with time since surgery, it is now better understood that significant overlap exists between the traditionally labeled acute and chronic rejection phases, with many forms of chronic active disease.

In light of the evolving nomenclature for allograft rejection, terms related to time from transplantation are still used in clinical practice. Hyperacute rejection can occur within minutes to hours but is usually identified in the operating room at the time of transplantation. This is a rare entity that involves abrupt global allograft nonperfusion and ischemia immediately after vascular anastomosis, secondary to small vessel thrombosis (Fig 13) (91,95). Hyperacute rejection results in a nonviable allograft requiring explantation.

Acute rejection occurs approximately 5–7 days after transplantation and is the result of T-cell activation (95). Accelerated acute rejection, which can occur in the first 5 postoperative days, is an antibody-mediated aggressive form of rejection that occurs in patients with a history of blood transfusion, prior transplantation, or other causes of presensitization (95). Chronic rejection involves gradual progressive deterioration

in allograft function, which can begin months to years after transplantation (91,95).

The imaging manifestations of rejection are nonspecific, highlighting the utility of protocol biopsy, which is used for definitive diagnosis. Still, US is often used in the workup to assess for other underlying causes of graft failure, such as nonspecific allograft nephropathy, drug toxicity, recurrent medical renal disease, renal vein thrombosis, uro-obstruction, and extrinsic compression of the allograft, all of which can result in deteriorated allograft function. At gray-scale US, features of rejection include edematous cortical thickening and loss of corticomedullary differentiation. Color Doppler US and spectral analysis may reveal diminished cortical flow and increased intraparenchymal arterial RIs (96).

Elevated intrarenal RI (>0.74), when measured in the early postoperative period between 1 week and 3 months, has been shown to correlate with diminished long-term function of the allograft at 1 year (97). The selected threshold used to determine what constitutes an elevated RI (0.75–0.80) influences the sensitivity and specificity of detecting acute rejection. Regardless, use of the RI alone does not allow reliable distinction between rejection and other causes of allograft dysfunction (98). Elevated RIs can be present in the setting of transplant rejection as well as ATN, nephrotoxic reactions to certain immunosuppressive agents (eg, tacrolimus or cyclosporine), ureteral obstruction, and mass effect on the allograft (eg, in the setting of extrinsic compression from a perinephric fluid collection) (99,100). Hence, knowledge of clinical history is vital during US assessment of the renal allograft.

Contrast-enhanced US allows evaluation of microvascular renal perfusion and can aid in predicting impending loss of renal function (101,102). In acute rejection, delayed cortical perfusion may be observed at contrast-enhanced US (103). Contrast-enhanced US can be implemented to sample the most viable areas of renal cortex at the time of biopsy (104).

CT is not usually performed in cases of suspected allograft rejection, as there is significant overlap between the appearance of rejection and ATN, both of which can demonstrate edematous enlargement of the allograft with patchy enhancement (91). MRI not only allows detailed depiction of renal transplant anatomy but also provides functional information. Diffusion-weighted imaging (DWI) has emerged as a promising noninvasive functional imaging technique for evaluation of renal allografts (105,106). BOLD (blood oxygenation level–dependent) and arterial spin labeling MRI techniques can provide information on allograft oxygenation and perfusion, which play a key role in evaluation of renal transplant function (106–108).

Acute Tubular Necrosis

Similar to allograft rejection, ATN is another important cause of early renal allograft dysfunction, and routine clinical assessment does not allow reliable distinction between the two entities. Radionuclide scintigraphy may be helpful but does not allow reliable differentiation between the two entities given overlapping findings, which typically include perfusion abnormalities and marked cortical retention with ^{99m}Tc MAG_3 (9). Use of fluorine 18 (^{18}F) fluorodeoxyglucose (FDG) PET/CT has been investigated for noninvasive differentiation between these two important diagnoses. However, percutaneous biopsy remains the standard of reference (109).

Drug-related Nephrotoxic Effects

Renal transplant immunosuppression regimens can be categorized into three phases or categories: induction therapy (intense immunosuppressive therapy immediately after transplantation), maintenance therapy, and treatment of rejection (110,111). Maintenance therapy can be comprised of antimetabolite agents (eg, azathioprine, mycophenolate mofetil), calcineurin inhibitors (eg, cyclosporine, tacrolimus), and corticosteroids (eg, oral prednisone) (111). In particular, calcineurin inhibitors, while known to have excellent short-term advantages, can result in chronic nephrotoxic effects with irreversible damage (112). Distinguishing between calcineurin inhibitor nephrotoxic effects and other causes of renal dysfunction remains a challenge.

Infectious Complications

Transplant recipients have a greater risk of infection owing to immunosuppression and may be susceptible to donor-related infections within the allograft. The KDIGO (Kidney Disease: Improving Global Outcomes) screening guidelines are designed to identify high-risk transplant donors and recipients to implement appropriate preventive measures, including administration of inactivated vaccines, therapeutic interventions, and specific monitoring protocols.

The types of bacterial, fungal, and viral infections that affect the renal transplant patient follow a relatively predictable pattern that correlates with the length of time from transplantation (Fig 2) (31). However, the pattern of timing of infections may vary significantly, depending on factors like net state of immunosuppression at different time points and choice and duration of antimicrobial prophylactic agents.

RadioGraphics

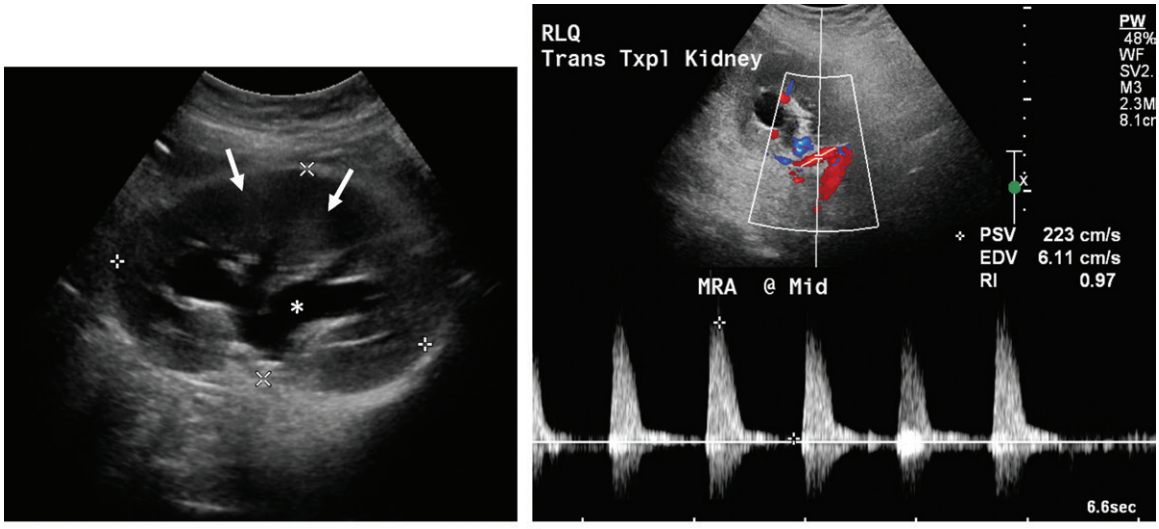

a. **b.**

Figure 14. BK virus nephropathy and hydronephrosis in a 69-year-old man 4 months after renal transplantation. **(a)** Gray-scale US image shows areas of mildly increased renal parenchymal echogenicity (arrows) and moderate hydronephrosis (*) without a visible obstructing intra- or extraluminal lesion at the renal pelvis. **(b)** Spectral Doppler image of the main renal artery shows relatively decreased diastolic flow and elevated RI. A nephroureteral stent was subsequently placed after nephrostography revealed stenosis of the transplant ureter at the anastomosis (not shown). Biopsy showed histopathologic findings of BK polyomavirus–associated nephropathy.

In the early phase (postoperative period to 1 month), most infections are related to surgery or are nosocomial and include antimicrobial-resistant bacteria such as methicillin-resistant *Staphylococcus aureus* (MRSA) and vancomycin-resistant enterococci (VRE) (31). The incidence of infections such as pneumonia, surgical wound infections, and urinary tract infections in renal transplant patients is comparable to those in non-immunocompromised patients who have undergone surgery (22). Donor-derived infections are rare during this period, and when they occur, are often viral (eg, herpes simplex virus, West Nile virus, rhabdovirus, and human immunodeficiency virus). Recipient-derived infections can occur as a result of colonized organisms (eg, *Aspergillus* or *Pseudomonas*) (31).

In the 2nd to 6th months after surgery, the transplant recipient is more susceptible to opportunistic infections, most commonly cytomegalovirus (CMV), which occurs in 8% of patients, followed by polyomavirus and Epstein-Barr virus (EBV) (31). Risk factors for development of infection during this period include seropositivity for a variety of viruses in either the donor or recipient and the extent to which the recipient is immunosuppressed. CMV and EBV are associated with a variety of renal transplant complications, which is part of the rationale for chemoprophylaxis in high-risk patients. In particular, screening for EBV in the 1st year is recommended in high-risk patients, as preemptive reduction of immunosuppression and early therapeutic intervention with drugs such as rituximab may reduce the incidence of posttransplant lymphoproliferative disorder (PTLD) (113), which is discussed later.

Another important infectious cause of renal allograft dysfunction or premature graft loss is polyomavirus nephropathy. BK virus is the predominant polyomavirus affecting renal transplant allografts, present in 5% of biopsy specimens (114). BK virus is an otherwise innocuous virus that is latent in an estimated 75% of the adult population, with some sources reporting estimates as high as 90% (115,116). Primary infection with BK virus is usually asymptomatic or associated with upper respiratory tract symptoms. BK virus can persist in a latent form in the kidney and urinary tract owing to its tendency to harbor genitourinary epithelium. The virus is more often donor derived and usually reactivates in the allograft within the first 3 months after transplantation, inducing tubulointerstitial inflammatory changes that may mimic acute cellular rejection (117).

The imaging appearance of BK virus nephropathy is still being described in the literature. Thus far, published imaging features associated with polyomavirus nephropathy include a streaky pattern of alternating hypoechoic bands at gray-scale US with increased RIs in the renal arteries at Doppler interrogation, signifying nonspecific nephritis (Fig 14). At contrast-enhanced CT, this may appear as areas of streaky or wedgelike hypoenhancement extending from the papilla to the cortex (118,119).

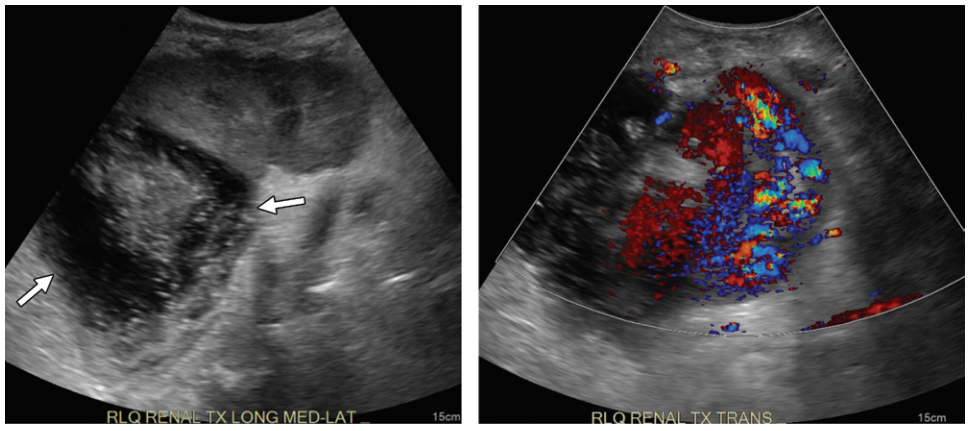

a. b.

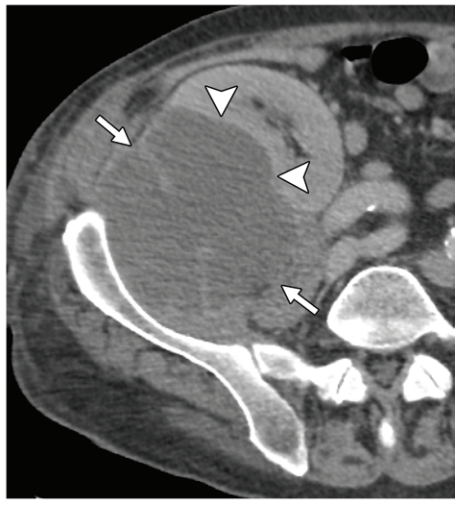

c.

Figure 15. *Nocardia* abscess in a 62-year-old man 2 months after deceased donor renal transplant. **(a)** Gray-scale US image shows a large complex perinephric collection (arrows) at the superior aspect of the transplant kidney. **(b)** Color Doppler image shows robust flow in the renal allograft without flow in the collection. **(c)** Axial contrast-enhanced CT image shows a multiseptated low-attenuation collection (arrows) deep to the superior aspect of the renal allograft, abutting the iliopsoas muscle medially and causing mass effect (arrowheads) on the transplant kidney. Culture of a specimen from CT-guided aspiration demonstrated *Nocardia* species.

High levels of viruria after transplantation are associated with hemorrhagic cystitis, ureteral obstruction, hydronephrosis, and renal allograft loss (116). In one study, obstructive uropathy was demonstrated in 83% of cases (120). Typically, the hydronephrosis in BK virus infection is mild to moderate (120). The ureteral obstruction may be due to urothelial edema and is often transient and reversible.

The standard of reference for diagnosis of BK virus–related nephropathy is renal biopsy, with specimens demonstrating varying degrees of tubular atrophy and fibrosis with inflammatory lymphocytic infiltrate (121). As with PTLD, initial treatment is reduction of immunosuppression, highlighting the importance of the immune system in regulating latent viral reactivation within the allograft. It is thought that improvement in immune function allows resolution of BK virus infection, which in turn results in resolution of BK virus–related upper urinary tract inflammation and ureteral stenosis (120). Temporary ureteral catheter placement can relieve the obstruction and improve renal function in the interim, with one group reporting a median time of 1 month before resolution of BK virus infection (120).

After 6 months, as the risk of early viral and latent infections diminishes, routine infections including community-acquired pneumonia and urinary tract infections are more commonly seen. However, as a result of continued immunosuppression, these patients remain at increased risk for opportunistic pathogens such as *Nocardia* and fungal organisms such as *Aspergillus* and *Mucor* species. *Nocardia* species are soil-borne gram-positive bacteria that are typically inhaled, first causing pulmonary nocardiosis, which can quickly disseminate to form multiorgan abscesses (Figs 15, 16) (122).

Imaging the allograft for evaluation of a transplant patient with suspected infection is aimed at excluding complications. At US, perinephric or parenchymal fluid collections with internal echogenic components and peripheral hypervascularity suggest the presence of an abscess. However, most often the appearance at US is normal, as seen with uncomplicated pyelonephritis in the native kidney. It is useful to evaluate the renal collecting system for the presence of any echogenic debris or mobile masses, which could represent pyonephrosis or a fungus ball, respectively (123).

At contrast-enhanced CT or MRI, a striated nephrogram can suggest pyelonephritis in a pa-

RadioGraphics

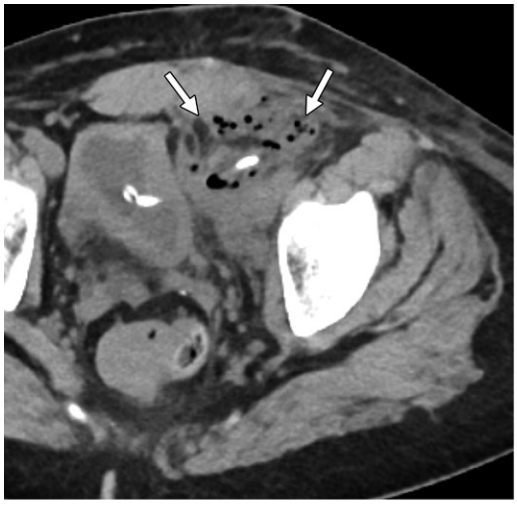

a.

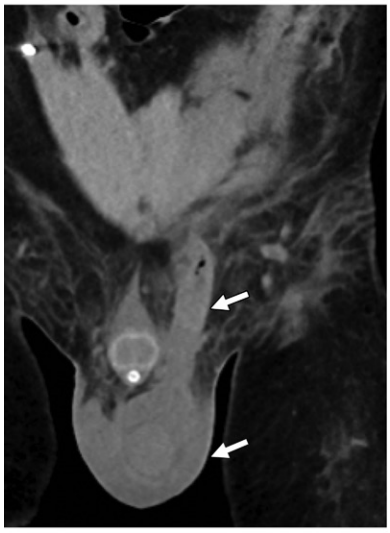

b.

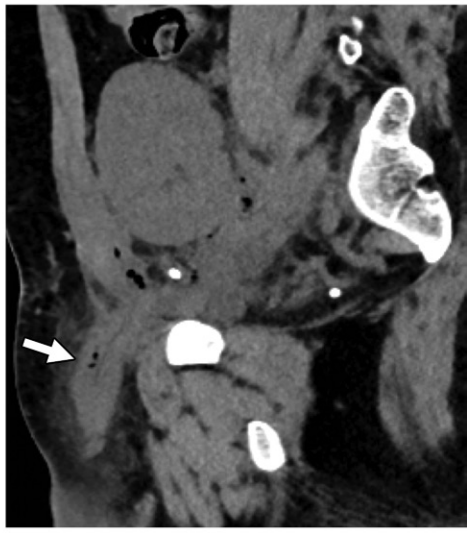

c.

Figure 16. Multiorganism perinephric abscess 17 days after left iliac fossa renal transplant in a 23-year-old man with spina bifida who presented with fever and penile swelling. **(a)** Axial nonenhanced CT image shows an ill-defined gas and fluid collection (arrows) inferior to the transplant kidney. **(b, c)** Coronal **(b)** and sagittal **(c)** nonenhanced CT images show extension of the gas and fluid collection into the left inguinal canal and scrotum (arrows). Exploration of the left iliac fossa revealed a perinephric abscess tracking into the scrotum, with cultures growing *Actinomyces* species and *Bacteroides fragilis*.

tient with fever, but may also be seen in obstructive uropathy and in the setting of renal vein thrombosis (124). Rarely, necrotizing infections within the renal allograft caused by gram-negative bacteria such as *Escherichia coli* may progress rapidly to emphysematous pyelonephritis, which may be life threatening and often requires allograft nephrectomy (Fig 17). Less than 30 cases of emphysematous pyelonephritis in a transplant kidney have been reported (125), but the severity of this complication warrants close attention for gas within the transplant kidney.

Neoplastic Complications

Malignancy is the third most common cause of death (after cardiovascular events and infection) in the renal transplant recipient, with three to five times the risk of malignancy as compared with the general population, with some cancers having markedly increased risk as high as 20–500-fold (15,126–128). Malignancy can occur as new malignancy in the recipient, as recurrent malignancy in the recipient, or as donor-related malignancy (transmitted to the recipient from the donor through the graft). The incidence and type of malignancy can vary between countries and time periods (15).

However, despite these heterogeneities between posttransplant populations, renal transplant recipients overall are predisposed to certain types of malignancies, with a distribution that is different from that of the general population. There is

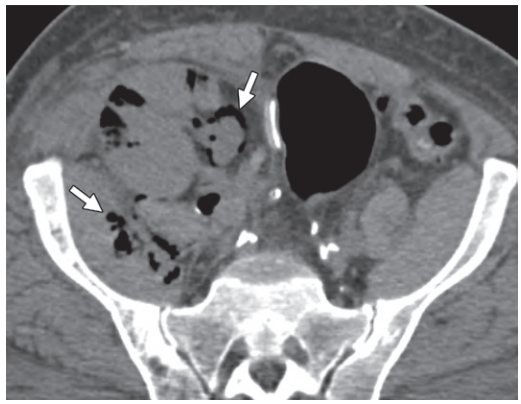

Figure 17. Acute emphysematous pyelonephritis in a 68-year-old man after deceased donor renal transplant 2 weeks earlier. Axial nonenhanced CT image shows abnormal gas replacing portions of the renal allograft parenchyma, with gas extending into the walls of the renal pelvis and perinephric spaces (arrows). Examination of the transplant nephrectomy specimen demonstrated necrotizing infection, cortical necrosis, and abscesses.

significantly increased incidence of some cancers (nonmelanomatous skin cancer, lymphoma, and colon cancer) and no increased incidence of others (breast, prostate, and brain cancers) (129). Annual dermatologic skin examination (and semiannual examinations in higher-risk patients, such as those with a history of squamous cell carcinoma [SCC] of the skin) and annual US or CT of the native kidneys have been suggested as recommended surveillance for skin cancers and native renal cell carcinomas (RCCs), respectively (15).

The renal allograft is susceptible to the same forms of malignancy known to occur in the native kidney, but also carries the additional risk for development of malignancies associated with chronic immunosuppression of the host and unregulated oncogenic viral infections (130). The risk of primary renal malignancy in the allograft overall is about six times that in the native kidney for all types, but substantially higher for papillary subtypes (13 times the general incidence) (Figs 18, 19) (131). Focused investigations of RCC in the allograft kidney have revealed a number of nuanced findings that suggest that the increased risk of malignancy is multifactorial, correlating with length of time receiving dialysis, form of preexisting native renal disease, race, and gender. Percutaneous radiofrequency ablation of RCC within the transplant kidney has been shown to be an effective therapy for low-grade tumors (T1a) without adverse effects on allograft function (132). An increased risk of urothelial malignancy has also been reported in renal transplant patients with BK virus infection (133).

PTLD is a common entity affecting post-transplant patients (126,134). Awareness of and heightened suspicion for this entity are important for diagnosis, particularly when assessing the allograft at surveillance imaging, as its presence may be clinically silent during the early stages, when it is most amenable to treatment. Treatment includes reduction of immunosuppression, which may result in complete resolution of the PTLD.

PTLD is less frequent in renal transplant patients as compared with lung, heart, and pancreas transplant patients, who require higher doses of immunosuppressive drugs (134). However, when it does occur in renal transplant patients, the renal allograft is the most common site of involvement (135). PTLD occurs in 1%–3% of renal transplant recipients (compared with up to 20% of non–renal allograft recipients) and can be nodal or extranodal. This disorder most often arises in the setting of active infection with Epstein-Barr virus (EBV) (also known as human herpesvirus 4) in the immunocompromised host and can range from mild polyclonal B-cell proliferation to diffuse multiorgan monoclonal lymphoma (136).

In more advanced stages of disease, solitary or multiple low-attenuation masses at CT involving the transplant kidney and other solid organs can be seen (Fig 20). In the renal allograft, there is a tendency for PTLD to manifest as a mass replacing or encasing the hilum, leading to outflow obstruction (134,136,137). In such cases, US, CT, and MRI may show allograft hydronephrosis with or without vascular encasement (134). PTLD lesions usually have low signal intensity on both T1- and T2-weighted MR images and show no significant enhancement. Increased FDG uptake is usually observed at PET/CT (134).

Screening renal transplant patients for cancer while they are on the transplant waiting list and after they have undergone transplantation is important. Minimizing doses of immunosuppressive drugs (as much as can be safely done) is also a key prevention strategy.

In rare instances, malignancy in the transplant recipient can develop as a result of clinically undetected donor-related cancer present in the renal allograft at the time of transplantation (Fig 21). The consequences of donor cancer transmission can be dramatic, with less than 50% survival rates for donor-related melanoma and lung cancer at 24 months after transplantation, a statistic that suggests that donors with a history of these

RadioGraphics

Figure 18. Allograft RCC with renal vein tumor thrombus in a 76-year-old man after deceased donor renal transplant 5 years earlier. **(a)** Coronal contrast-enhanced arterial phase CT image shows a heterogeneously enhancing mass (*) in the upper transplant kidney, with distortion of the expected corticomedullary enhancement pattern in this region. Note the enhancing soft tissue in the transplant renal vein (arrow). **(b)** Duplex US image of the expansile thrombus in the transplant renal vein shows an arterial waveform, consistent with a malignant tumor thrombus. **(c)** Gray-scale (left) and microbubble-enhanced (right) US images show expansile echogenic soft tissue filling the main renal vein (* in left image) with corresponding avid enhancement (arrow in right image), consistent with tumor thrombus in the main renal vein.

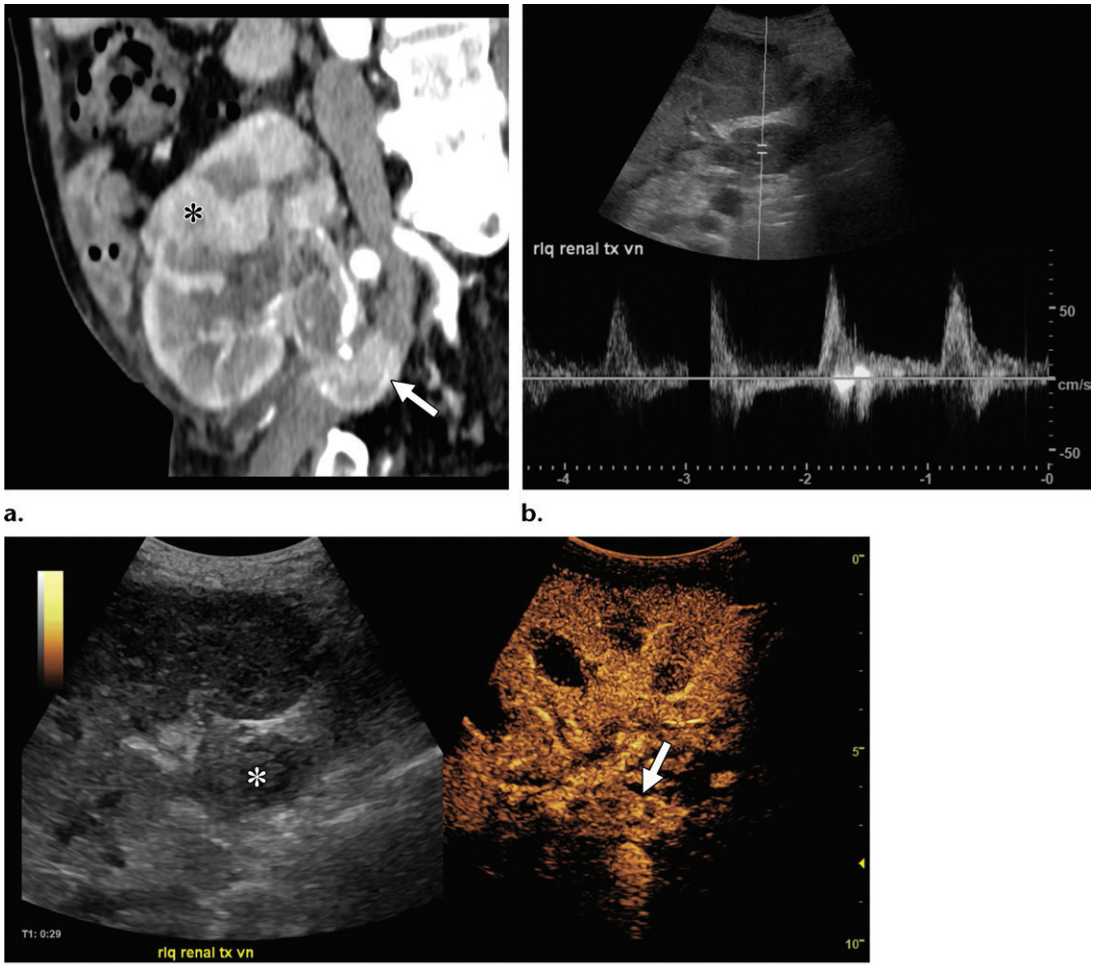

types of malignancies should be precluded from the donor pool (138). As prognosis varies depending on the type of donor-related malignancy, there is need for continued investigation into the risk and benefits of accepting kidneys from donors with a history of cancer, depending on cancer type, histologic stage at time of diagnosis, and disease-free interval before transplantation (139). Nevertheless, this complication remains rare. A review of 17 639 donors in the United Kingdom Transplant Registry, including 202 patients with a history of cancer, found no cases of donor cancer transmission at 10 years (140).

Routine surveillance imaging plays an important role in early detection of cancer in the renal allograft. Elevated intraparenchymal arterial RIs may be the only initial indication of an underlying abnormality, which may prompt biopsy or further diagnostic imaging that may reveal an unsuspected malignancy (Fig 22).

Future Directions

Efforts to safely increase the available supply and utilization of existing donor kidneys on the basis of evidence-based data are ongoing. The Collaborative Innovation and Improvement Network (COIIN) is a UNOS (United Network for Organ Sharing)–sponsored project aimed at supporting greater use of deceased donor kidneys with moderate to high KDPI (kidney donor profile index) scores (>50%).

Allograft rejection remains a challenging problem in renal transplant recipients despite continued advances in immunosuppressive therapy. While percutaneous needle biopsy remains the reference standard for diagnosis of acute allograft

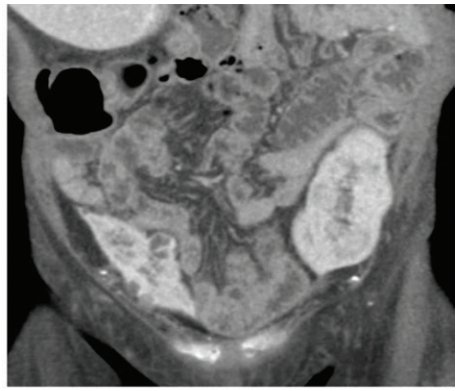

a.

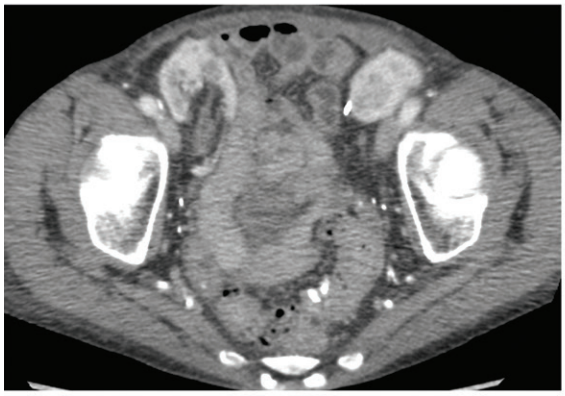

b.

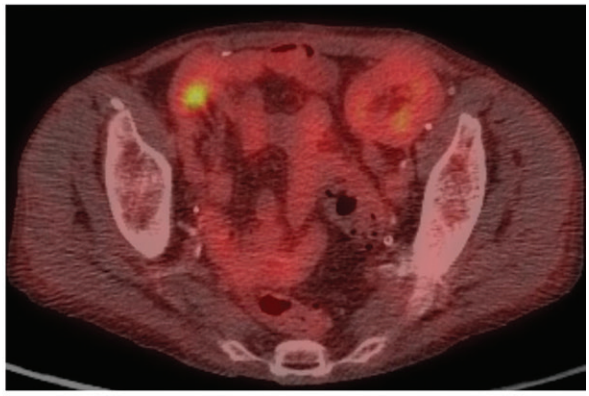

c.

Figure 19. Multifocal clear cell renal cell tubulopapillary renal cell carcinoma in a failed deceased donor allograft in a 66-year-old woman after right lower quadrant kidney transplant 12 years earlier. **(a)** Coronal contrast-enhanced CT image shows a small failed transplant kidney in the right iliac fossa, with a complex cystic partially exophytic hypovascular mass with a thick enhancing septum in the interpolar region. Note the normal transplant kidney in the left iliac fossa. **(b, c)** Axial contrast-enhanced CT image **(b)** and corresponding ^{18}F-FDG PET/CT image **(c)** show an additional small hypoenhancing mass with abnormal increased radiotracer uptake.

a.

b.

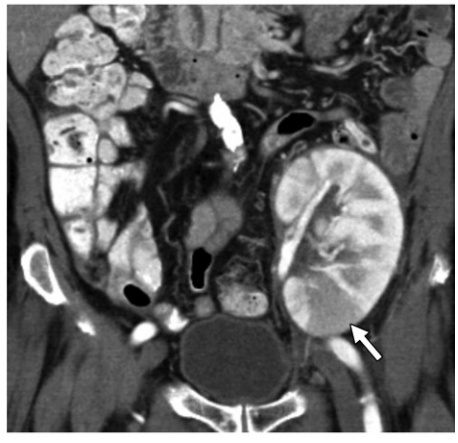

c.

Figure 20. PTLD in a 78-year-old man after deceased donor renal transplant 5 months earlier. **(a)** Gray-scale US image 2 months after surgery shows normal appearance of the allograft. **(b)** Gray-scale US image from 5-month surveillance imaging shows diffuse somewhat lobulated enlargement of the renal parenchyma with loss of corticomedullary differentiation. **(c)** Coronal contrast-enhanced CT image shows a focal ill-defined hypoattenuating soft-tissue mass (arrow) in the lower pole of the allograft parenchyma. Immunohistochemical analysis of a biopsy specimen (not shown) revealed predominantly λ-restricted plasma cell infiltrate, which in conjunction with positive FISH (fluorescence in situ hybridization) results for Epstein-Barr virus confirmed the diagnosis of PTLD.

RadioGraphics

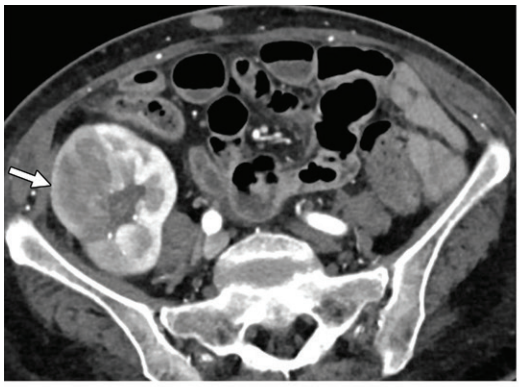

a.

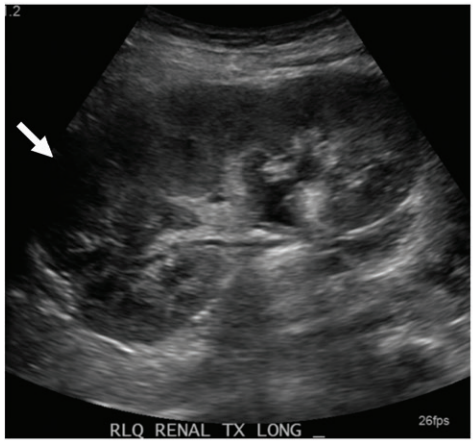

b.

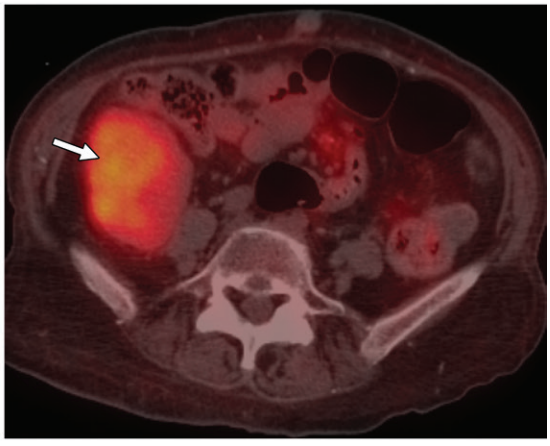

c.

Figure 21. Donor-derived allograft squamous cell carcinoma (SCC) in a 72-year-old woman after expanded-criteria deceased donor renal transplant 11 months earlier. **(a)** Axial contrast-enhanced CT image shows a hypoenhancing infiltrative mass (arrow) in the upper transplant kidney. **(b)** Longitudinal US image shows a heterogeneous ill-defined mass (arrow) centered at the upper pole of the allograft with distortion of the renal contour. **(c)** Axial ^{18}F-FDG PET/CT image shows masslike hypermetabolism in the allograft (arrow). Biopsy showed SCC originating from a male donor, confirmed by an XY signal pattern in the tumor nuclei in this female patient. She developed pulmonary metastases and died less than 3 years after transplantation.

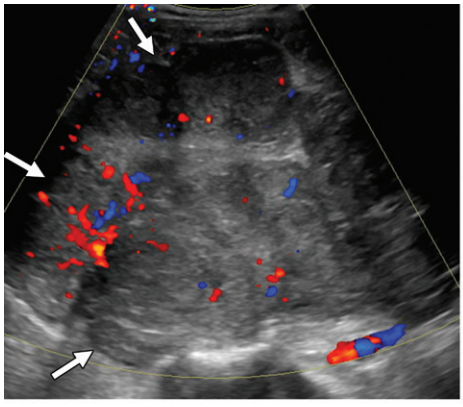

a.

b.

c.

Figure 22. Low-grade myxoid spindle cell neoplasm in a 29-year-old man with a history of chronic glomerulonephritis who presented with new-onset hypertension after living donor renal transplant 15 years earlier. **(a)** Color Doppler image shows a heterogeneous mass with internal vascularity (arrows) that replaces the renal allograft, with loss of identifiable renal architecture. **(b)** Axial contrast-enhanced CT image shows a large, lobulated, heterogeneously enhancing mass (arrows) in the right lower abdomen at the expected site of the transplant kidney. **(c)** Photograph of the gross pathology specimen shows a lobulated mucinous neoplasm, which was confirmed to be a low-grade myxoid spindle cell neoplasm.

rejection, new noninvasive imaging techniques aimed at detecting early signs of rejection may allow greater specificity in selecting which patients should ultimately undergo biopsy. Microbubble contrast-enhanced US is a diagnostic tool with promising applications in the renal transplant patient population, combining the general advantages of standard US (eg, lack of ionizing radiation, cost-effectiveness, and wide availability) with the advantage of a contrast agent that does not require renal filtration (141).

Given the accepted pathophysiology of decreased cortical blood flow in acute rejection–related inflammation, a quantitative technique using contrast-enhanced US to analyze dynamic renal enhancement characteristics has been proposed as a noninvasive index for predicting acute rejection (96). Additional techniques based on tissue elastography and T-lymphocyte antibody-labeled microbubble contrast-enhanced US are also being investigated. Contrast-enhanced US may have an additional role as a problem-solving tool in evaluation of indeterminate renal lesions, particularly for differentiating complicated cysts and solid renal neoplasms.

Conclusion

Complications of renal transplantation continue to evolve alongside the changing landscape of improving surgical techniques, immunosuppression regimens, surveillance imaging, and overall understanding of rejection. Duplex US is the primary tool for routine surveillance and initial diagnostic imaging for allograft dysfunction. Advanced imaging techniques including MRI and contrast-enhanced US can be used as adjuncts to traditional duplex US and renal allograft biopsy in workup of posttransplant complications.

Acknowledgments.—Many thanks to Margaret (Maggie) Ryan, MD, for her guidance on transplant kidney histopathologic analysis and rejection. Special thanks to Aaron Laviana, MD, for insights into transplant surgical technique. We also wish to thank all the dedicated transplant surgeons, nephrologists, and members of the multidisciplinary transplant teams at the Mayo Clinic and Emory University School of Medicine for their commitment to the highest-quality care for our renal transplant patients.

***Disclosures of Conflicts of Interest.*—N.D.** *Activities related to the present article:* disclosed no relevant relationships. *Activities not related to the present article:* consultant for GE Healthcare. *Other activities:* disclosed no relevant relationships.

References

1. Organ Procurement and Transplantation Network. National data. https://optn.transplant.hrsa.gov/data/view-data-reports/national-data/#. Published 2019. Accessed January 28, 2019.
2. Merion RM, Ashby VB, Wolfe RA, et al. Deceased-donor characteristics and the survival benefit of kidney transplantation. JAMA 2005;294(21):2726–2733.
3. Organ Procurement and Transplantation Network. Kidney donor profile index (KDPI) for clinicians. https://optn.transplant.hrsa.gov/resources/guidance/kidney-donor-profile-index-kdpi-guide-for-clinicians/. Published 2019. Accessed January 28, 2019.
4. Hariharan S, Johnson CP, Bresnahan BA, Taranto SE, McIntosh MJ, Stablein D. Improved graft survival after renal transplantation in the United States, 1988 to 1996. N Engl J Med 2000;342(9):605–612.
5. Wang JH, Skeans MA, Israni AK. Current status of kidney transplant outcomes: dying to survive. Adv Chronic Kidney Dis 2016;23(5):281–286.
6. Wilkinson A. Protocol transplant biopsies: are they really needed? Clin J Am Soc Nephrol 2006;1(1):130–137.
7. Horrow MM, Parsikia A, Zaki R, Ortiz J. Immediate postoperative sonography of renal transplants: vascular findings and outcomes. AJR Am J Roentgenol 2013;201(3):W479–W486.
8. Granata A, Clementi S, Londrino F, et al. Renal transplant vascular complications: the role of Doppler ultrasound. J Ultrasound 2014;18(2):101–107.
9. el Maghraby TA, van Eck-Smit BL, de Fijter JW, Pauwels EK. Quantitative scintigraphic parameters for the assessment of renal transplant patients. Eur J Radiol 1998;28(3):256–269.
10. Aktas A, Aras M, Colak T, Gencoglu A, Karakayali H. Comparison of Tc-99m DTPA and Tc-99m MAG3 perfusion time-activity curves in patients with renal allograft dysfunction. Transplant Proc 2006;38(2):449–453.
11. Taylor AT. Radionuclides in nephrourology. II. Pitfalls and diagnostic applications. J Nucl Med 2014;55(5):786–798.
12. Kasiske BL, Zeier MG, Chapman JR, et al. KDIGO clinical practice guideline for the care of kidney transplant recipients: a summary. Kidney Int 2010;77(4):299–311.
13. Matas AJ, Smith JM, Skeans MA, et al. OPTN/SRTR 2011 annual data report: kidney. Am J Transplant 2013;13(suppl 1):11–46.
14. Kasiske BL, Vazquez MA, Harmon WE, et al; American Society of Transplantation. Recommendations for the outpatient surveillance of renal transplant recipients. J Am Soc Nephrol 2000;11(suppl 15):S1–S86.
15. Morath C, Mueller M, Goldschmidt H, Schwenger V, Opelz G, Zeier M. Malignancy in renal transplantation. J Am Soc Nephrol 2004;15(6):1582–1588.
16. Campsen J, Bang TJ, Kam I, Gupta R. May-Thurner syndrome complicating left-sided renal transplant. Transplantation 2010;89(7):904–906.
17. Breda A, Territo A, Gausa L, et al. Robot-assisted kidney transplantation: the European experience. Eur Urol 2018;73(2):273–281.
18. Modi P, Pal B, Modi J, et al. Retroperitoneoscopic living-donor nephrectomy and laparoscopic kidney transplantation: experience of initial 72 cases. Transplantation 2013;95(1):100–105.
19. Troppmann C, Wiesmann K, McVicar JP, Wolfe BM, Perez RV. Increased transplantation of kidneys with multiple renal arteries in the laparoscopic live donor nephrectomy era: surgical technique and surgical and nonsurgical donor and recipient outcomes. Arch Surg 2001;136(8):897–907.
20. Ooms LS, Roodnat JI, Dor FJ, et al. Kidney retransplantation in the ipsilateral iliac fossa: a surgical challenge. Am J Transplant 2015;15(11):2947–2954.
21. Becker BN, Odorico JS, Becker YT, et al. Simultaneous pancreas-kidney and pancreas transplantation. J Am Soc Nephrol 2001;12(11):2517–2527.
22. Akbar SA, Jafri SZ, Amendola MA, Madrazo BL, Salem R, Bis KG. Complications of renal transplantation. RadioGraphics 2005;25(5):1335–1356.
23. Sugi MD, Albadawi H, Knuttinen G, et al. Transplant artery thrombosis and outcomes. Cardiovasc Diagn Ther 2017;7(suppl 3):S219–S227.
24. Saidi R, Kawai T, Kennealey P, et al. Living donor kidney transplantation with multiple arteries: recent increase in modern era of laparoscopic donor nephrectomy. Arch Surg 2009;144(5):472–475.
25. Al-Katib S, Shetty M, Jafri SM, Jafri SZ. Radiologic assessment of native renal vasculature: a multimodality review. RadioGraphics 2017;37(1):136–156.
26. Pal DK, Sanki PK, Roy S. Analysis of outcome of end-to-end and end-to-side internal iliac artery anastomosis in renal

transplantation: our initial experience with a case series. Urol Ann 2017;9(2):166–169.
27. Fananapazir G, Tse G, Corwin MT, et al. Pediatric en bloc kidney transplants: clinical and immediate postoperative US factors associated with vascular thrombosis. Radiology 2016;279(3):935–942.
28. Keller AK, Jorgensen TM, Jespersen B. Identification of risk factors for vascular thrombosis may reduce early renal graft loss: a review of recent literature. J Transplant 2012;2012:793461.
29. Penna FJ, Lorenzo AJ, Farhat WA, Butt H, Koyle MA. Ureteroureterostomy: an alternative to ureteroneocystostomy in select cases of pediatric renal transplantation. J Urol 2017;197(3 Pt 2):920–924.
30. Norris JM, Ravi-Shankar S, Klimach SG. Urinary reconstruction after kidney transplantation: pyeloureterostomy versus ureteroneocystostomy. Int J Surg 2015;19:83–86.
31. Fishman JA. Infection in organ transplantation. Am J Transplant 2017;17(4):856–879.
32. Reyna-Sepúlveda F, Ponce-Escobedo A, Guevara-Charles A, et al. Outcomes and surgical complications in kidney transplantation. Int J Organ Transplant Med 2017;8(2):78–84.
33. Ortiz J, Parsikia A, Horrow MM, Khanmoradi K, Campos S, Zaki R. Risk factors for renal allograft compartment syndrome. Int Surg 2014;99(6):851–856.
34. Ball CG, Kirkpatrick AW, Yilmaz S, Monroy M, Nicolaou S, Salazar A. Renal allograft compartment syndrome: an underappreciated postoperative complication. Am J Surg 2006;191(5):619–624.
35. Nguan CY, Beasley KA, McAlister VC, Luke PP. Treatment of renal transplant complications with a mesh hood fascial closure technique. Am J Surg 2007;193(1):119–121.
36. Thiyagarajan UM, Bagul A, Mohamed I, Nicholson ML. Post-biopsy renal allograft compartment syndrome: addressing the problem, illustrated with a case report. Int J Surg Case Rep 2011;2(7):188–190.
37. Morgan TA, Chandran S, Burger IM, Zhang CA, Goldstein RB. Complications of ultrasound-guided renal transplant biopsies. Am J Transplant 2016;16(4):1298–1305.
38. Lubner MG, Simard ML, Peterson CM, Bhalla S, Pickhardt PJ, Menias CO. Emergent and nonemergent nonbowel torsion: spectrum of imaging and clinical findings. RadioGraphics 2013;33(1):155–173.
39. Patel MD, Phillips CJ, Young SW, et al. US-guided renal transplant biopsy: efficacy of a cortical tangential approach. Radiology 2010;256(1):290–296.
40. Laberge JM. Interventional management of renal transplant arteriovenous fistula. Semin Intervent Radiol 2004;21(4):239–246.
41. Patel MD, Young SW, Scott Kriegshauser J, Dahiya N. Ultrasound-guided renal transplant biopsy: practical and pragmatic considerations. Abdom Radiol (NY) 2018;43(10):2597–2603.
42. Baffour FI, Hickson LJ, Stegall MD, et al. Effects of aspirin therapy on ultrasound-guided renal allograft biopsy bleeding complications. J Vasc Interv Radiol 2017;28(2):188–194.
43. Furness PN, Philpott CM, Chorbadjian MT, et al. Protocol biopsy of the stable renal transplant: a multicenter study of methods and complication rates. Transplantation 2003;76(6):969–973.
44. Perini S, Gordon RL, LaBerge JM, et al. Transcatheter embolization of biopsy-related vascular injury in the transplant kidney: immediate and long-term outcome. J Vasc Interv Radiol 1998;9(6):1011–1019.
45. Saad NE, Saad WE, Davies MG, Waldman DL, Fultz PJ, Rubens DJ. Pseudoaneurysms and the role of minimally invasive techniques in their management. RadioGraphics 2005;25(suppl 1):S173–S189.
46. Liu X, Berg N, Sheehan J, et al. Renal transplant: nonenhanced renal MR angiography with magnetization-prepared steady-state free precession. Radiology 2009;251(2):535–542.
47. Brown ED, Chen MY, Wolfman NT, Ott DJ, Watson NE Jr. Complications of renal transplantation: evaluation with US and radionuclide imaging. RadioGraphics 2000;20(3):607–622.
48. Kolofousi C, Stefanidis K, Cokkinos DD, Karakitsos D, Antypa E, Piperopoulos P. Ultrasonographic features of kidney transplants and their complications: an imaging review. ISRN Radiol 2012;2013:480862.
49. Hanbidge AE, Buckler PM, O'Malley ME, Wilson SR. From the RSNA refresher courses: imaging evaluation for acute pain in the right upper quadrant. RadioGraphics 2004;24(4):1117–1135.
50. Joshi G, Crawford KA, Hanna TN, Herr KD, Dahiya N, Menias CO. US of right upper quadrant pain in the emergency department: diagnosing beyond gallbladder and biliary disease. RadioGraphics 2018;38(3):766–793.
51. Fananapazir G, Rao R, Corwin MT, Naderi S, Santhanakrishnan C, Troppmann C. Sonographic evaluation of clinically significant perigraft hematomas in kidney transplant recipients. AJR Am J Roentgenol 2015;205(4):802–806.
52. Alonso RC, Nacenta SB, Martinez PD, Guerrero AS, Fuentes CG. Kidney in danger: CT findings of blunt and penetrating renal trauma. RadioGraphics 2009;29(7):2033–2053.
53. Park SB, Kim JK, Cho KS. Complications of renal transplantation: ultrasonographic evaluation. J Ultrasound Med 2007;26(5):615–633.
54. Kobayashi K, Censullo ML, Rossman LL, Kyriakides PN, Kahan BD, Cohen AM. Interventional radiologic management of renal transplant dysfunction: indications, limitations, and technical considerations. RadioGraphics 2007;27(4):1109–1130.
55. Tulchinsky M, Malpani AR, Eggli DF. Diagnosis of urinoma by MAG3 scintigraphy in a renal transplant patient. Clin Nucl Med 1995;20(1):80–81.
56. Titton RL, Gervais DA, Hahn PF, Harisinghani MG, Arellano RS, Mueller PR. Urine leaks and urinomas: diagnosis and imaging-guided intervention. RadioGraphics 2003;23(5):1133–1147.
57. Richard HM. Perirenal transplant fluid collections. Semin Intervent Radiol 2004;21(4):235–237.
58. Ranghino A, Segoloni GP, Lasaponara F, Biancone L. Lymphatic disorders after renal transplantation: new insights for an old complication. Clin Kidney J 2015;8(5):615–622.
59. Zietek Z, Sulikowski T, Tejchman K, et al. Lymphocele after kidney transplantation. Transplant Proc 2007;39(9):2744–2747.
60. Bzoma B, Kostro J, Debska-Slizien A, et al. Treatment of the lymphocele after kidney transplantation: a single-center experience. Transplant Proc 2016;48(5):1637–1640.
61. Ayvazoglu Soy EH, Akdur A, Kirnap M, Boyvat F, Moray G, Haberal M. Vascular complications after renal transplant: a single-center experience. Exp Clin Transplant 2017;15(suppl 1):79–83.
62. Srivastava A, Kumar J, Sharma S, Abhishek, Ansari MS, Kapoor R. Vascular complication in live related renal transplant: an experience of 1945 cases. Indian J Urol 2013;29(1):42–47.
63. Kiykim AA, Ozer C, Yildiz A, et al. Development of transplant renal artery thrombosis and signs of haemolytic-uraemic syndrome following the change from cyclosporin to tacrolimus in a renal transplant patient. Nephrol Dial Transplant 2004;19(10):2653–2656.
64. McCarthy JM, Yeung CK, Keown PA. Late renal-artery thrombosis after transplantation associated with intraoperative abdominopelvic compression. N Engl J Med 1990;323(26):1845.
65. Ponticelli C, Moia M, Montagnino G. Renal allograft thrombosis. Nephrol Dial Transplant 2009;24(5):1388–1393.
66. Browne RF, Tuite DJ. Imaging of the renal transplant: comparison of MRI with duplex sonography. Abdom Imaging 2006;31(4):461–482.
67. Sharfuddin A. Renal relevant radiology: imaging in kidney transplantation. Clin J Am Soc Nephrol 2014;9(2):416–429.
68. McDonald RA, Smith JM, Stablein D, Harmon WE. Pretransplant peritoneal dialysis and graft thrombosis following pediatric kidney transplantation: a NAPRTCS report. Pediatr Transplant 2003;7(3):204–208.
69. Singh A, Stablein D, Tejani A. Risk factors for vascular thrombosis in pediatric renal transplantation: a special report of the North American Pediatric Renal Transplant Cooperative Study. Transplantation 1997;63(9):1263–1267.
70. Lockhart ME, Wells CG, Morgan DE, Fineberg NS, Robbin ML. Reversed diastolic flow in the renal transplant:

perioperative implications versus transplants older than 1 month. AJR Am J Roentgenol 2008;190(3):650–655.
71. Clarke SD, Kennedy JA, Hewitt JC, McEvoy J, McGeown MG, Nelson SD. Successful removal of thrombus from renal vein after renal transplantation. BMJ 1970;1(5689): 154–155.
72. Misra P, Kirpalani A, Leung G, et al. The role of thrombectomy and diffusion-weighted imaging with MRI in post-transplant renal vein thrombosis: a case report. BMC Nephrol 2017;18(1):224.
73. Bruno S, Remuzzi G, Ruggenenti P. Transplant renal artery stenosis. J Am Soc Nephrol 2004;15(1):134–141.
74. de Morais RH, Muglia VF, Mamere AE, et al. Duplex Doppler sonography of transplant renal artery stenosis. J Clin Ultrasound 2003;31(3):135–141.
75. Robinson KA, Kriegshauser JS, Dahiya N, Young SW, Czaplicki CD, Patel MD. Detection of transplant renal artery stenosis: determining normal velocities at the renal artery anastomosis. Abdom Radiol (NY) 2017;42(1):254–259.
76. Patel U, Khaw KK, Hughes NC. Doppler ultrasound for detection of renal transplant artery stenosis: threshold peak systolic velocity needs to be higher in a low-risk or surveillance population. Clin Radiol 2003;58(10):772–777.
77. Morrow KL, Kim AH, Plato SA 2nd, et al. Increased risk of renal dysfunction with percutaneous mechanical thrombectomy compared with catheter-directed thrombolysis. J Vasc Surg 2017;65(5):1460–1466.
78. Fananapazir G, McGahan JP, Corwin MT, et al. Screening for transplant renal artery stenosis: ultrasound-based stenosis probability stratification. AJR Am J Roentgenol 2017;209(5):1064–1073.
79. Moresco KP, Patel NH, Namyslowski Y, Shah H, Johnson MS, Trerotola SO. Carbon dioxide angiography of the transplanted kidney: technical considerations and imaging findings. AJR Am J Roentgenol 1998;171(5):1271–1276.
80. Karam G, Hétet JF, Maillet F, et al. Late ureteral stenosis following renal transplantation: risk factors and impact on patient and graft survival. Am J Transplant 2006;6(2):352–356.
81. Kumar S, Ameli-Renani S, Hakim A, Jeon JH, Shrivastava S, Patel U. Ureteral obstruction following renal transplantation: causes, diagnosis and management. Br J Radiol 2014;87(1044):20140169.
82. Sandhu C, Patel U. Renal transplantation dysfunction: the role of interventional radiology. Clin Radiol 2002;57(9): 772–783.
83. Kriegshauser JS, Naidu SG, Heilman RL, et al. Primary percutaneous treatment of transplant ureteral strictures using tandem stents. J Vasc Interv Radiol 2013;24(6):874–880.
84. Abdul-Muhsin HM, McAdams SB, Nuñez RN, Katariya NN, Castle EP. Robot-assisted transplanted ureteral stricture management. Urology 2017;105:197–201.
85. Jeon H, McHugh PP, Ranjan D, Johnston TD, Gedaly R, Pu LL. Successful management of eviscerated renal allograft with preservation of function. Am J Transplant 2008;8(5):1067–1070.
86. Levine MA, Schuler T, Gourishankar S. Complications in the 90-day postoperative period following kidney transplant and the relationship of the Charlson Comorbidity Index. Can Urol Assoc J 2017;11(12):388–393.
87. Miura Y, Sato K, Kawagishi N, Ohuchi N. Strangulated small bowel obstruction after renal transplant with no history of laparotomy: case report. Exp Clin Transplant 2015;13(3):295–297.
88. Hanssen O, Erpicum P, Lovinfosse P, et al. Non-invasive approaches in the diagnosis of acute rejection in kidney transplant recipients. I. In vivo imaging methods. Clin Kidney J 2017;10(1):97–105.
89. Kawashima A, Sandler CM, Corl FM, et al. Imaging of renal trauma: a comprehensive review. RadioGraphics 2001;21(3):557–574.
90. Moore EE, Moore FA. American Association for the Surgery of Trauma organ injury scaling: 50th anniversary review article of the Journal of Trauma. J Trauma 2010;69(6):1600–1601.
91. Kim N, Juarez R, Levy AD. Imaging non-vascular complications of renal transplantation. Abdom Radiol (NY) 2018;43(10):2555–2563.
92. Humar A, Ramcharan T, Kandaswamy R, Gillingham K, Payne WD, Matas AJ. Risk factors for slow graft function after kidney transplants: a multivariate analysis. Clin Transplant 2002;16(6):425–429.
93. Ojo AO, Wolfe RA, Held PJ, Port FK, Schmouder RL. Delayed graft function: risk factors and implications for renal allograft survival. Transplantation 1997;63(7):968–974.
94. Haas M, Loupy A, Lefaucheur C, et al. The Banff 2017 Kidney Meeting report: revised diagnostic criteria for chronic active T cell-mediated rejection, antibody-mediated rejection, and prospects for integrative endpoints for next-generation clinical trials. Am J Transplant 2018;18(2):293–307.
95. Bhowmik DM, Dinda AK, Mahanta P, Agarwal SK. The evolution of the Banff classification schema for diagnosing renal allograft rejection and its implications for clinicians. Indian J Nephrol 2010;20(1):2–8.
96. Thölking G, Schuette-Nuetgen K, Kentrup D, Pawelski H, Reuter S. Imaging-based diagnosis of acute renal allograft rejection. World J Transplant 2016;6(1):174–182.
97. McArthur C, Geddes CC, Baxter GM. Early measurement of pulsatility and resistive indexes: correlation with long-term renal transplant function. Radiology 2011;259(1):278–285.
98. Allen KS, Jorkasky DK, Arger PH, et al. Renal allografts: prospective analysis of Doppler sonography. Radiology 1988;169(2):371–376.
99. Venz S, Kahl A, Hierholzer J, et al. Contribution of color and power Doppler sonography to the differential diagnosis of acute and chronic rejection, and tacrolimus nephrotoxicity in renal allografts. Transpl Int 1999;12(2):127–134.
100. Friedewald SM, Molmenti EP, Friedewald JJ, Dejong MR, Hamper UM. Vascular and nonvascular complications of renal transplants: sonographic evaluation and correlation with other imaging modalities, surgery, and pathology. J Clin Ultrasound 2005;33(3):127–139.
101. Benozzi L, Cappelli G, Granito M, et al. Contrast-enhanced sonography in early kidney graft dysfunction. Transplant Proc 2009;41(4):1214–1215.
102. Schwenger V, Hinkel UP, Nahm AM, Morath C, Zeier M. Real-time contrast-enhanced sonography in renal transplant recipients. Clin Transplant 2006;20(suppl 17):51–54.
103. Zeisbrich M, Kihm LP, Drüschler F, Zeier M, Schwenger V. When is contrast-enhanced sonography preferable over conventional ultrasound combined with Doppler imaging in renal transplantation? Clin Kidney J 2015;8(5):606–614.
104. Kazmierski B, Deurdulian C, Tchelepi H, Grant EG. Applications of contrast-enhanced ultrasound in the kidney. Abdom Radiol (NY) 2018;43(4):880–898.
105. Blondin D, Lanzman RS, Klasen J, et al. Diffusion-attenuated MRI signal of renal allografts: comparison of two different statistical models. AJR Am J Roentgenol 2011;196(6):W701–W705.
106. Thoeny HC, Zumstein D, Simon-Zoula S, et al. Functional evaluation of transplanted kidneys with diffusion-weighted and BOLD MR imaging: initial experience. Radiology 2006;241(3):812–821.
107. Artz NS, Sadowski EA, Wentland AL, et al. Arterial spin labeling MRI for assessment of perfusion in native and transplanted kidneys. Magn Reson Imaging 2011;29(1): 74–82.
108. Sadowski EA, Fain SB, Alford SK, et al. Assessment of acute renal transplant rejection with blood oxygen level–dependent MR imaging: initial experience. Radiology 2005;236(3):911–919.
109. Lovinfosse P, Weekers L, Bonvoisin C, et al. Fluorodeoxyglucose F(18) positron emission tomography coupled with computed tomography in suspected acute renal allograft rejection. Am J Transplant 2016;16(1):310–316.
110. Kalluri HV, Hardinger KL. Current state of renal transplant immunosuppression: present and future. World J Transplant 2012;2(4):51–68.
111. Halloran PF. Immunosuppressive drugs for kidney transplantation. N Engl J Med 2004;351(26):2715–2729.
112. Naesens M, Kuypers DR, Sarwal M. Calcineurin inhibitor nephrotoxicity. Clin J Am Soc Nephrol 2009;4(2):481–508.
113. Morton M, Coupes B, Roberts SA, et al. Epstein-Barr virus infection in adult renal transplant recipients. Am J Transplant 2014;14(7):1619–1629.

114. Nickeleit V, Singh HK, Randhawa P, et al. The Banff Working Group Classification of Definitive Polyomavirus Nephropathy: morphologic definitions and clinical correlations. J Am Soc Nephrol 2018;29(2):680–693.
115. Lamarche C, Orio J, Collette S, et al. BK polyomavirus and the transplanted kidney: immunopathology and therapeutic approaches. Transplantation 2016;100(11):2276–2287.
116. Raval M, Gulbis A, Bollard C, et al. Evaluation and management of BK virus-associated nephropathy following allogeneic hematopoietic cell transplantation. Biol Blood Marrow Transplant 2011;17(11):1589–1593.
117. Bohl DL, Brennan DC. BK virus nephropathy and kidney transplantation. Clin J Am Soc Nephrol 2007;2(suppl 1):S36–S46.
118. Dugo M, Mangino M, Meola M, et al. Ultrasound findings of BK polyomavirus-associated nephropathy in renal transplant patients. J Nephrol 2017;30(3):449–453.
119. Tourret J, Mercadal L, Penna RR, Brochériou I, Barrou B. Visualizing BK virus nephropathy. NDT Plus 2010;3(2):185–186.
120. Khan H, Oberoi S, Mahvash A, et al. Reversible ureteral obstruction due to polyomavirus infection after percutaneous nephrostomy catheter placement. Biol Blood Marrow Transplant 2011;17(10):1551–1555.
121. Sawinski D, Goral S. BK virus infection: an update on diagnosis and treatment. Nephrol Dial Transplant 2015;30(2):209–217.
122. Bargehr J, Flors L, Leiva-Salinas C, et al. Nocardiosis in solid-organ transplant recipients: spectrum of imaging findings. Clin Radiol 2013;68(5):e266–e271.
123. Kale H, Narlawar RS, Rathod K. Renal fungal ball: an unusual sonographic finding. J Clin Ultrasound 2002;30(3):178–180.
124. Saunders HS, Dyer RB, Shifrin RY, Scharling ES, Bechtold RE, Zagoria RJ. The CT nephrogram: implications for evaluation of urinary tract disease. RadioGraphics 1995;15(5):1069–1085; discussion 1086–1088.
125. Narcisse D, Agarwal M, Hancock M, Wells D, Sands C. A rare case of emphysematous pyelonephritis in a renal transplant patient. Ther Adv Infect Dis 2016;3(6):141–144.
126. Zeier M, Hartschuh W, Wiesel M, Lehnert T, Ritz E. Malignancy after renal transplantation. Am J Kidney Dis 2002;39(1):E5.
127. Briggs JD. Causes of death after renal transplantation. Nephrol Dial Transplant 2001;16(8):1545–1549.
128. Einollahi B, Rostami Z, Nourbala MH, et al. Incidence of malignancy after living kidney transplantation: a multicenter study from Iran. J Cancer 2012;3:246–256.
129. Sprangers B, Nair V, Launay-Vacher V, Riella LV, Jhaveri KD. Risk factors associated with post-kidney transplant malignancies: an article from the Cancer-Kidney International Network. Clin Kidney J 2018;11(3):315–329.
130. Katabathina VS, Menias CO, Tammisetti VS, et al. Malignancy after solid organ transplantation: comprehensive imaging review. RadioGraphics 2016;36(5):1390–1407.
131. Karami S, Colt JS, Stewart PA, et al. A case-control study of occupational sunlight exposure and renal cancer risk. Int J Cancer 2016;138(7):1626–1633.
132. Cool DW, Kachura JR. Radiofrequency ablation of T1a renal cell carcinomas within renal transplant allografts: oncologic outcomes and graft viability. J Vasc Interv Radiol 2017;28(12):1658–1663.
133. Hickman LA, Sawinski D, Guzzo T, Locke JE. Urologic malignancies in kidney transplantation. Am J Transplant 2018;18(1):13–22.
134. Camacho JC, Moreno CC, Harri PA, Aguirre DA, Torres WE, Mittal PK. Posttransplantation lymphoproliferative disease: proposed imaging classification. RadioGraphics 2014;34(7):2025–2038.
135. Rajiah P, Lim YY, Taylor P. Renal transplant imaging and complications. Abdom Imaging 2006;31(6):735–746.
136. Vrachliotis TG, Vaswani KK, Davies EA, Elkahammas EA, Bennett WF, Bova JG. CT findings in posttransplantation lymphoproliferative disorder of renal transplants. AJR Am J Roentgenol 2000;175(1):183–188.
137. Ali MG, Coakley FV, Hricak H, Bretan PN. Complex posttransplantation abnormalities of renal allografts: evaluation with MR imaging. Radiology 1999;211(1):95–100.
138. Xiao D, Craig JC, Chapman JR, Dominguez-Gil B, Tong A, Wong G. Donor cancer transmission in kidney transplantation: a systematic review. Am J Transplant 2013;13(10):2645–2652.
139. Feng S, Buell JF, Cherikh WS, et al. Organ donors with positive viral serology or malignancy: risk of disease transmission by transplantation. Transplantation 2002;74(12):1657–1663.
140. Desai R, Collett D, Watson CJ, Johnson P, Evans T, Neuberger J. Estimated risk of cancer transmission from organ donor to graft recipient in a national transplantation registry. Br J Surg 2014;101(7):768–774.
141. Mori G, Granito M, Favali D, Cappelli G. Long-term prognostic impact of contrast-enhanced ultrasound and power Doppler in renal transplantation. Transplant Proc 2015;47(7):2139–2141.